

Organozirconium Complexes as Catalysts for Markovnikov-Selective Intermolecular Hydrothiolation of Terminal Alkynes: Scope and Mechanism

Charles J. Weiss and Tobin J. Marks*

Department of Chemistry, Northwestern University, Evanston, Illinois 60208

Received May 10, 2010; E-mail: t-marks@northwestern.edu

Abstract: The efficient and selective organozirconium(IV)-mediated, intermolecular hydrothiolation of terminal alkynes by aliphatic, benzylic, and aromatic thiols using CGCZrMe₂ (CGC = Me₂SiCp'' NCM₃, Cp'' = C₅Me₄), Cp*ZrBn₃ (Cp* = C₅Me₅, Bn = benzyl), Cp*ZrCl₂NMe₂, Cp*₂ZrMe₂, and Zr(NMe₂)₄ precatalysts is reported. These transformations are shown to be highly Markovnikov-selective, with selectivities up to 99%, and typically in greater than 90% yields. The reaction has been demonstrated on the preparative scale with 72% isolated yield and 99% Markovnikov selectivity. A mixture of anti-Markovnikov products is occasionally observed as a result of a known, non-organometallic, radical mechanism, which can be suppressed by addition of a radical inhibitor. Kinetic investigations show that the CGCZrMe₂-mediated reaction between 1-pentanethiol and 1-hexyne is first-order in catalyst concentration, first-order in alkyne concentration, and also first-order in thiol at lower concentrations but transitions to zero-order at concentrations > 0.3 M. Deuterium labeling of the alkyne yields $k_4/k_0 = 1.3(0.1)$, along with evidence of thiol-mediated protonolytic detachment of product from the Zr center. Activation parameters for CGCZrMe₂-mediated 1-pentanethiol hydrothiolation of 1-hexyne measured over the temperature range of 50–80 °C are $\Delta H^\ddagger = +18.1(1.2)$ kcal/mol and $\Delta S^\ddagger = -20.9(2.5)$ e.u. for [alkyne] and [thiol] at 0.2 M. These and other findings are consistent with turnover-limiting alkyne insertion into the Zr–SR bond, followed by a thiol-induced Zr–C protonolysis. Observed zirconium–thiolate dimers in the reaction medium suggest instances of dimeric catalyst resting states and possible aggregated, hydrothiolation-active species.

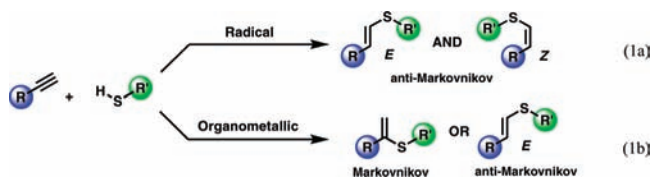
Introduction

Sulfur is a significant component in many natural products,¹ chemical reagents,² and synthetic materials,³ creating the need for efficient and selective means of incorporating sulfur into organic frameworks. Hydrothiolation is an atom-economical method for the formation of C–S bonds and can be achieved via a variety of pathways including radical⁴ and catalytic

processes.^{2a,5} Radical hydrothiolation yields unselective mixtures of *E* and *Z* vinyl sulfides (eq 1a) while organometallic catalysts offer access to Markovnikov vinyl sulfides or *E* anti-Markovnikov vinyl sulfides (eq 1b) with varying degrees of turnover and selectivity.^{2a,5,6} Note that while diverse variants of organometallic complex-mediated hydroelementation⁷ have been extensively explored, including hydroamination,⁸ hydrophosphination,⁹ and hydroalkoxylation,¹⁰ only recently has hydrothiola-

- (1) (a) Meng, D.; Chen, W.; Zhao, W. *J. Nat. Prod.* **2007**, *70*, 824–829. (b) Zhang, Y.; Liu, S.; Che, Y.; Liu, X. *J. Nat. Prod.* **2007**, *70*, 1522–1525. (c) Nicolaou, K. C.; Sorensen, E. J. *Classics in Total Synthesis*; Wiley-VHC: New York, 1996.
- (2) (a) Sabarre, A.; Love, J. *Org. Lett.* **2008**, *10*, 3941–3944. (b) Yus, M.; Guti rrez, A.; Foubelo, F. *Tetrahedron* **2001**, *57*, 4411–4422. (c) Foubelo, F.; Guti rrez, A.; Yus, M. *Tetrahedron Lett.* **1999**, *40*, 8173–8176. (d) Metzner, P.; Thuillier, A., *Sulfur Reagents in Organic Synthesis*; Academic Press: San Diego, 1994. (e) Belen'kii, L. I. *Chemistry of Organosulfur Compounds*; Ellis Horwood: New York, 1990. (f) de Lucchi, O.; Pasquato, L. *Tetrahedron* **1988**, *44*, 6755–6794.
- (3) (a) Kloxin, C. J.; Scott, T. F.; Bowman, C. N. *Macromolecules* **2009**, *42*, 2551–2556. (b) Konkolewicz, D.; Gray-Weale, A.; Perrier, S. b *J. Am. Chem. Soc.* **2009**, *131*, 18075–18077. (c) San Miguel, L.; Matzger, A. J. *Macromolecules* **2007**, *40*, 9233–9237. (d) Valdebenito, A.; Encinas, M. V. *Polymer* **2005**, *46*, 10658–10662. (e) Roncali, J. *Chem. Rev.* **1992**, *92*, 711–738.
- (4) (a) Capella, L.; Montecchi, P. C.; Navacchia, M. L. *J. Org. Chem.* **1996**, *61*, 6783–6789. (b) Benati, L.; Capella, L.; Montecchi, P. C.; Spagnolo, P. J. *Chem. Soc., Perkin Trans.* **1995**, 1035–1038. (c) Benati, L.; Montecchi, P. C.; Spagnolo, P. J. *Chem. Soc., Perkin Trans.* **1991**, 2103–2109. (d) Ichinose, Y.; Wakamatsu, K.; Nozaki, K.; Birbaum, J.-L.; Oshima, K.; Utimoto, K. *Chem. Lett.* **1987**, *16*, 1647–1650. (e) Griesbaum, K. *Angew. Chem., Int. Ed. Engl.* **1970**, *9*, 273–287.

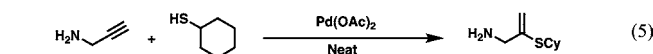
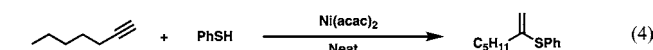
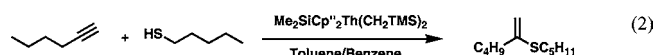
- (5) (a) Corma, A.; Gonz lez-Arellano, C.; Iglesias, M.; S nchez, F. *Appl. Catal., A* **2010**, *375*, 49–54. (b) Ananikov, V. P.; Gayduk, K. A.; Orlov, N. V.; Beletskaya, I. P.; Khrustalev, V. N.; Antipin, M. Y. *Chem.–Eur. J.* **2010**, *16*, 2063–2071. (c) Shoai, S.; Bichler, P.; Kang, B.; Buckley, H.; Love, J. A. *Organometallics* **2007**, *26*, 5778–5781. (d) Kondoh, A.; Yorimitsu, H.; Oshima, K. *Org. Lett.* **2007**, *9*, 1383–1385. (e) Fraser, L. R.; Bird, J.; Wu, Q.; Cao, C.; Patrick, B. O.; Love, J. A. *Organometallics* **2007**, *26*, 5602–5611. (f) Delp, S. A.; Munro-Leighton, C.; Goj, L. A.; Ramirez, M. A.; Gunnoe, T. B.; Petersen, J. L.; Boyle, P. D. *Inorg. Chem.* **2007**, *46*, 2365–2367. (g) Beletskaya, I. P.; Ananikov, V. P. *Pure Appl. Chem.* **2007**, *79*, 1041–1056. (h) Beletskaya, I. P.; Ananikov, V. P. *Eur. J. Org. Chem.* **2007**, 3431–3444. (i) Ananikov, V. P.; Orlov, N. V.; Beletskaya, I. P.; Khrustalev, V. N.; Antipin, M. Y.; Timofeeva, T. V. *J. Am. Chem. Soc.* **2007**, *129*, 7252–7253. (j) Malyshev, D. A.; Scott, N. M.; Marion, N.; Stevens, E. D.; Ananikov, V. P.; Beletskaya, I. P.; Nolan, S. P. *Organometallics* **2006**, *25*, 4462–4470. (k) Ananikov, V. P.; Zaleskiy, S. S.; Orlov, N. V.; Beletskaya, I. P. *Russ. Chem. Bull.* **2006**, *55*, 2109–2113. (l) Ananikov, V. P.; Orlov, N. V.; Beletskaya, I. P. *Organometallics* **2006**, *25*, 1970–1977. (m) Cao, C.; Fraser, L. R.; Love, J. A. *J. Am. Chem. Soc.* **2005**, *127*, 17614–17615. (n) Ananikov, V. P.; Malyshev, D. A.; Beletskaya, I. P.; Aleksandrov, G. G.; Eremenko, I. L. *Adv. Synth. Catal.* **2005**, *347*, 1993–2001. (o) Kondo, T.; Mitsudo, T. *Chem. Rev.* **2000**, *100*, 3205–3220.



tion^{2a,5,8,11} been investigated in detail due to the historic reputation of sulfur as a catalyst poison,^{5a,12} reflecting its high affinity for ‘soft’ transition metal centers.¹³

Interest in homogeneous, catalytic alkyne hydrothiolation over the past few years has yielded a number of metal complexes competent to effect this transformation using late transition metal^{2a,5,8b,14} and actinide¹¹ catalysts. Late transition metal catalysts include Rh,^{2a,5c,e,m,6,8b,14a} Ir,^{8b} Ni,^{5b,g,h,j–l,n} Pd,^{5b,g,i,14} Pt,^{5g} and Au^{5a} complexes while actinide investigations have

employed organo-Th(IV) and organo-U(IV) complexes.¹¹ While some late transition metal catalysts exhibit high activity, achieving high Markovnikov selectivity still presents a challenge, with the exception of Pd, as does competing isomerization of the alkene product,^{13a} double-thiolation products,^{5j} and product insertion into a second alkyne.^{5j,15} Furthermore, while some late transition metal complexes effect efficient alkyne hydrothiolation with benzyl and aryl thiols, few mediate hydrothiolation with the less reactive aliphatic thiols.^{5c,d,i,m} Actinide complexes have demonstrated impressive hydrothiolation selectivity and the ability to utilize aliphatic thiols (e.g., eq 2);¹¹ however the non-negligible radioactivity may render them undesirable for large-scale use. Previous work with rhodium catalysts demonstrated the ability to utilize both terminal and internal alkynes with selectivity typically favoring the linear (*E*) anti-Markovnikov products (e.g., eq 3)^{5c} with the exception of Tp*Rh(PPh₃)₂ where Markovnikov vinyl sulfides are selectively produced.^{5m} Studies on group 10 metals find that nickel (e.g., eq 4)^{5l} and palladium (e.g., eq 5)⁵ⁱ catalysts favor the Markovnikov product.



Available mechanistic data for late transition metal- and organoactinide-mediated hydrothiolation complexes are consistent with pathways in which the alkyne undergoes insertion into either a metal–hydride or metal–thiolate bond.^{5c,h,j,11,14a} The accepted hydride pathway for most Rh complexes^{5c,14a} is initiated by π -coordination/activation of the acetylene to/by the metal–hydride complex (Scheme 1A, step *i*), followed by alkyne insertion into the Rh–H bond (Scheme 1A, step *ii*). Finally, regeneration of the catalyst occurs through reductive elimination of product followed by RS–H oxidative addition to the metal center (Scheme 1A, step *iii*). Rhodium complexes selectively yield *E* anti-Markovnikov products as a result of the hydride insertion regiochemistry. In contrast, Pd,^{5h,14a} Ni,^{5h,j} and Th¹¹ complexes are proposed to effect hydrothiolation via acetylene insertion into the metal–thiolate bond (Scheme 1B, step *i*) followed by thiol-mediated displacement of product from the metal center (Scheme 1B, step *ii*), resulting in Markovnikov selectivity.

The recently communicated activity of organoactinides for alkyne hydrothiolation¹¹ and the efficacy of inexpensive organozirconium complexes¹⁶ for formally analogous hydroamination processes^{8a,f,k,m,17} raises the question as to whether, and with what activity and selectivity, zirconium(IV) complexes

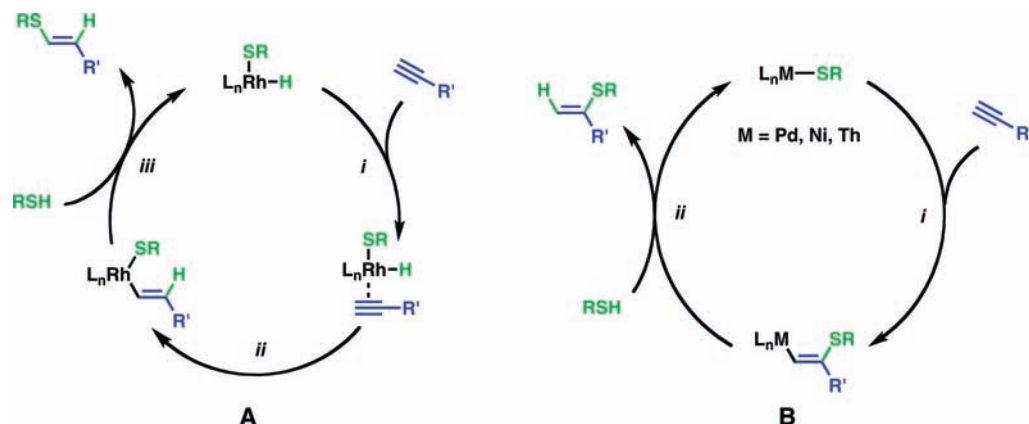
- (6) Misumi, Y.; Seino, H.; Mizobe, Y. *J. Organomet. Chem.* **2006**, *691*, 3157–3164.
- (7) (a) Hartwig, J. F. *Nature* **2008**, *455*, 314–322. (b) Andrea, T.; Eisen, M. S. *Chem. Soc. Rev.* **2008**, *37*, 550–567. (c) Alonso, F.; Beletskaya, I. P.; Yus, M. *Chem. Rev.* **2004**, *104*, 3079–3160. (d) Togni, A.; Grutzmacher, H.-J. *Catalytic Heterofunctionalization*; Wiley-VCH: New York, 2001.
- (8) (a) Leitch, D. C.; Payne, P. R.; Dunbar, C. R.; Schafer, L. L. *J. Am. Chem. Soc.* **2009**, *131*, 18246–18247. (b) Field, L. D.; Messerle, B. A.; Vuong, K. Q.; Turner, P. *Dalton Trans.* **2009**, 3599–3614. (c) Reznichenko, A. L.; Hampel, F.; Hultsch, K. C. *Chem.—Eur. J.* **2009**, *15*, 12819–12827. (d) Müller, T. E.; Hultsch, K. C.; Yus, M.; Foubelo, F.; Tada, M. *Chem. Rev.* **2008**, *108*, 3795–3892. (e) Munro-Leighton, C.; Delp, S. A.; Alsop, N. M.; Blue, E. D.; Gunnoe, T. B. *Chem. Commun.* **2008**, 111–113. (f) Smolensky, E.; Kapon, M.; Eisen, M. S. *Organometallics* **2007**, *26*, 4510–4527. (g) Motta, A.; Fragalà, I. L.; Marks, T. J. *Organometallics* **2006**, *25*, 5533–5539. (h) Hong, S.; Marks, T. J. *Acc. Chem. Res.* **2004**, *37*, 673–686. (i) Motta, A.; Lanza, G.; Fragalà, I. L.; Marks, T. J. *Organometallics* **2004**, *23*, 4097–4104. (j) Ryu, J.-S.; Li, G. Y.; Marks, T. J. *J. Am. Chem. Soc.* **2003**, *125*, 12584–12605. (k) Ackermann, L.; Bergman, R. G.; Loy, R. N. *J. Am. Chem. Soc.* **2003**, *125*, 11956–11963. (l) Ryu, J. S.; Li, G. Y.; Marks, T. J. *J. Am. Chem. Soc.* **2003**, *125*, 12584–12605. (m) Arredondo, V. M.; McDonald, F. E.; Marks, T. J. *Organometallics* **1999**, *18*, 1949–1960. (n) Walsh, P. J.; Baranger, A. M.; Bergman, R. G. *J. Am. Chem. Soc.* **1992**, *114*, 1708–1719.
- (9) (a) Perrier, A.; Comte, V.; Moise, C.; Le Gendre, P. *Chem.—Eur. J.* **2009**, *16*, 64–67. (b) Nagata, S.; Kawaguchi, S.-i.; Matsumoto, M.; Kamiya, I.; Nomoto, A.; Sonoda, M.; Ogawa, A. *Tetrahedron Lett.* **2007**, *48*, 6637–6640. (c) Motta, A.; Fragalà, I. L.; Marks, T. J. *Organometallics* **2005**, *24*, 4995–5003. (d) Sadow, A. D.; Haller, I.; Fadini, L.; Togni, A. *J. Am. Chem. Soc.* **2004**, *126*, 14704–14705. (e) Takaki, K.; Koshiji, G.; Komeyama, K.; Takeda, M.; Shishido, T.; Kitani, A.; Takehira, K. *J. Org. Chem.* **2003**, *68*, 6554–6565. (f) Kawaoaka, A. M.; Douglass, M. R.; Marks, T. J. *Organometallics* **2003**, *22*, 4630–4632. (g) Douglass, M. R.; Stern, C. L.; Marks, T. J. *J. Am. Chem. Soc.* **2001**, *123*, 10221–10238. (h) Douglass, M. R.; Marks, T. J. *J. Am. Chem. Soc.* **2000**, *122*, 1824–1825. (i) Wicht, D. K.; Kourkine, I. V.; Lew, B. M.; Nthenge, J. M.; Glueck, D. S. *J. Am. Chem. Soc.* **1997**, *119*, 5039–5040.
- (10) (a) Dzudza, A.; Mark, T. J. *Chem.—Eur. J.* **2010**, *16*, 3403–3422. (b) Motta, A.; Fragalà, I. L.; Marks, T. J. *Organometallics* **2010**, *29*, 2004–2012. (c) Nishina, N.; Yamamoto, Y. *Tetrahedron* **2009**, *65*, 1799–1808. (d) Janini, T. E.; Rakosi, R. I.; Durr, C. B.; Bertke, J. A.; Bunge, S. D. *Dalton Trans.* **2009**, 10601–10608. (e) Dzudza, A.; Marks, T. J. *Org. Lett.* **2009**, *11*, 1523–1526. (f) Cui, D.-M.; Yu, K.-R.; Zhang, C. *Synlett* **2009**, 7, 1103–1106. (g) Seo, S.; Yu, X.; Marks, T. J. *J. Am. Chem. Soc.* **2009**, *131*, 263–276. (h) Nishina, N.; Yamamoto, Y. *Tetrahedron Lett.* **2008**, *49*, 4908–4911. (i) Zhang, Z.; Widenhofer, R. A. *Org. Lett.* **2008**, *10*, 2079–2081. (j) Harkat, H.; Weibel, J.-M.; Pale, P. *Tetrahedron Lett.* **2007**, *48*, 1439–1442. (k) Yu, X.; Seo, S.; Marks, T. J. *J. Am. Chem. Soc.* **2007**, *129*, 7244–7245. (l) Zhang, Z.; Liu, C.; Kinder, R. E.; Han, X.; Qian, H.; Widenhofer, R. A. *J. Am. Chem. Soc.* **2006**, *128*, 9066–9073. (m) Yang, C. G.; Reich, N. W.; Shi, Z.; He, C. *Org. Lett.* **2005**, *7*, 4553–4556. (n) Qian, H.; Han, X.; Widenhofer, R. A. *J. Am. Chem. Soc.* **2004**, *126*, 9536–9537.
- (11) Weiss, C. J.; Wobser, S. D.; Marks, T. J. *J. Am. Chem. Soc.* **2009**, *131*, 2062–2063.
- (12) Hegedus, L. L.; McCabe, R. W. *Chemical Industries Series, Vol. 17: Catalyst Poisoning*; 1984.

- (13) (a) Stephan, D. W.; Nadasdi, T. T. *Coord. Chem. Rev.* **1996**, *147*, 147–208. (b) Krebs, B.; Henkel, G. *Angew. Chem., Int. Ed. Engl.* **1991**, *30*, 769–788.

- (14) (a) Ogawa, A.; Ikeda, T.; Kimura, K.; Hirao, T. *J. Am. Chem. Soc.* **1999**, *121*, 5108–5114. (b) Kuniyasu, H.; Ogawa, A.; Sato, K.; Ryu, I.; Kambe, N.; Sonoda, N. *J. Am. Chem. Soc.* **1992**, *114*, 5902–5903.

- (15) After the insertion of alkyne into the Pd–SR bond (Scheme 1B, step *i*), the insertion of a second alkyne into the Pd–vinyl bond occurs instead of the release of product from the metal center (Scheme 1B, step *ii*) resulting in a diene sulfide.

Scheme 1. Proposed Alkyne Hydrothiolation Mechanisms for Late Transition Metal and Actinide Complexes



might be competent to mediate hydrothiolation. In past instances of organozirconium-mediated alkyne hydroamination,^{8a,m,17a} Markovnikov selectivity similar to that of f-element catalysts has been observed,^{8h,j} suggesting that organozirconium complexes may offer a selective, catalytic route to Markovnikov vinyl sulfides. Herein, we report the first implementation of organozirconium complexes for the Markovnikov-selective, catalytic hydrothiolation of a broad variety of terminal alkynes by aliphatic, benzylic, and aromatic thiols. This includes efficient routes to Markovnikov vinyl sulfides with a wide range of thiols and terminal alkynes. In addition, detailed mechanistic studies probe the pathway by which this transformation occurs via kinetic analysis, substituent effects, and deuterium-labeling studies.

Experimental Section

Materials and Methods. Due to the air and moisture sensitivity of the organozirconium complexes used in this study, all manipulations were carried out in oven-dried, Schlenk-type glassware interfaced to either a dual-manifold Schlenk line, high-vacuum line (10^{-6} Torr), or in a nitrogen-filled glovebox (<1 ppm O_2). Argon (Airgas) was further purified by passing through columns of MnO and activated 4Å Davison molecular sieves immediately before use. Toluene for preparative scale and benzene- d_6 (Cambridge Isotope Laboratories, 99+ atom % D) for NMR reactions and kinetic measurements were stored over Na/K alloy *in vacuo* and vacuum transferred immediately prior to use or were stored in a nitrogen-filled glovebox until use. Diethylether for synthesis was distilled from Na/benzophenone immediately prior to use. Thiols and alkynes were purchased from Aldrich, VWR, GFS Chemicals, and Acros; they were distilled and transferred across multiple beds of activated Davison 4Å molecular sieves as solutions in benzene- d_6 or neat, followed by degassing (10^{-6} Torr) via freeze–pump–thaw methods. All substrates were stored under argon until use. Conjugated alkynes and thiols were stored at -10 °C until use. Ethanethiol- d (98 atom % D) was prepared according to literature methods,¹¹ and D_2O was purchased from Cambridge Isotope Laboratories (99.9 atom % D). The organozirconium precatalysts CGCZrMe₂ (**1**),¹⁸ Cp*ZrBn₃ (**2**),¹⁹ and Cp*ZrCl₂NMe₂ (**3**)²⁰ were prepared as reported

in the literature, while Zr[NMe₂]₄ (**5**) was purchased from Aldrich and used as received. The methyltriphenylsilane ¹H NMR internal integration standard for kinetic studies was purchased from Strem, sublimed under high vacuum, and stored in a glovebox until use. NMR spectroscopic data for products **12**, **14**, **19**, **21**, **29**, and **31** agree with the published literature spectra.^{5m,11,21}

Physical and Analytical Measurements. NMR spectra were recorded on Mercury 400 (400 MHz, ¹H; 100 MHz, ¹³C; 61 MHz, ²H) and Avance III 500 (500 MHz, ¹H; 125 MHz, ¹³C) NMR spectrometers. Chemical shifts (δ) are referenced relative to internal solvent resonances and reported relative to Me₄Si. Spectra of air-sensitive reactions and materials were taken in airtight, Teflon-valved J. Young NMR tubes. Samples were heated in silicon oil baths with the temperature controlled by an Ika ETS-D4 probe. GC data were collected on an HP6890 GC-MS equipped with an HP5972 detector and an HP-5MS (5% phenyl methyl siloxane, 30 m \times 250 μ m \times 0.25 μ m) capillary column while high-resolution mass spectra were collected on an Agilent 6210 LC-TOF (ESI, APPI) and Thermo Finnegan MAT900 (EI).

Typical NMR-Scale Catalytic Reaction. In a glovebox, CGCZrMe₂ (**1**, 3.7 mg, 10 μ mol) and methyltriphenylsilane (8.0 mg, 29.5 μ mol) were dissolved in 0.6 mL of C₆D₆ and added to a J. Young NMR tube. The tube was sealed, removed from the glovebox, and attached to a high-vacuum line where 0.2 mL of thiol and 0.2 mL of alkyne solutions (both 1.0 M in benzene- d_6 ; 0.2 mmol; 20-molar excess) were syringed in under an argon flush. The reaction mixture was then sealed, shaken well, degassed by a single freeze–pump–thaw cycle, and placed in a preheated, temperature-controlled oil bath covered with aluminum foil.

Kinetic Experiments. The same procedure as described above was followed except that the sample was periodically cooled to room temperature to collect ¹H NMR spectra.²² Turnover frequency (N_T) was determined by the method of initial rate²³ where data points were collected early in the reaction before the substrates had been appreciably consumed (see Supporting Information). As a result, the reaction during this period of time can be approximated as pseudo-zero-order with respect to the substrate concentrations, resulting in a linear trend. The resulting linear plots were fit by a

- (16) (a) Marek, I. *New Aspects of Zirconium Containing Organic Compounds*; Springer: Berlin, New York, 2005. (b) Marek, I. *Titanium and zirconium in organic synthesis*; Wiley-VCH: Weinheim, 2002. (c) Hey-Hawkins, E. *Chem. Rev.* **1994**, *94*, 1661–1717. (d) Poli, R. *Chem. Rev.* **1991**, *91*, 509–551. (e) Cardin, D. J.; Lappert, M. F.; Raston, C. L. *Chemistry of Organo-Zirconium and -Hafnium Compounds*; Halsted Press: New York, 1986.
- (17) (a) Majumder, S.; Odom, A. L. *Organometallics* **2008**, *27*, 1174–1177. (b) Stubbert, B. D.; Marks, T. J. *J. Am. Chem. Soc.* **2007**, *129*, 6149–6167.

- (18) Carpenetti, D. W.; Kloppenburg, L.; Kupec, J. T.; Petersen, J. L. *Organometallics* **1996**, *15*, 1572–1581.
- (19) Wolczanski, P. T.; Bercaw, J. E. *Organometallics* **1982**, *1*, 793–799.
- (20) Irigoyen, A. M.; Martin, A.; Mena, M.; Palacios, F.; Yelamos, C. J. *Organomet. Chem.* **1995**, *494*, 255–259.
- (21) Fiandanese, V.; Marchese, G.; Naso, F.; Ronzini, L. *Synthesis* **1987**, 1034–1036.
- (22) To test for temperature-dependent mechanism changes, samples were tested at constant temperature without the repeated heating/cooling and showed results consistent with those which were repeatedly heated/cooled. Additionally, no change in the catalyst or substrates were observed as a result of the heating/cooling cycles.

linear-regression analysis using $R^2 \geq 0.99$ according to eq 6, and N_t was calculated according to eq 7 where $[\text{catalyst}]_0$ = initial concentration of precatalyst and t = time in h. Kinetic experiments in this study were performed at 0.2 M [thiol] and [alkyne] unless otherwise indicated. Linear corrections for slight variations in initial [thiol] and [alkyne] were applied as needed.

$$[\text{product}] = mt \quad (6)$$

$$N_t (\text{h}^{-1}) = \frac{m}{[\text{catalyst}]_0} \quad (7)$$

Yield and Selectivity Measurements. In the glovebox, Cp^*ZrBn_3 (**2**, 5.0 mg, 10 μmol) was dissolved in 0.4 mL of C_6D_6 and the resulting solution was transferred to a J. Young NMR tube. The tube was then sealed, removed from the glovebox, and attached to the high-vacuum line where 0.2 mL of thiol and 0.6 mL of alkyne solutions (both 1.0 M in benzene- d_6 ; 0.2 mmol; 20 molar excess in thiol) were syringed in under an argon flush. The reaction mixture was then sealed, shaken well, degassed by a single freeze–pump–thaw cycle, and placed in a temperature-controlled, 120 °C oil bath for 24.0 h. The product conversion and selectivity were determined by ^1H NMR and GC/MS.

General Procedure for Purification of Products. After carrying out NMR-scale reactions as described above, the reaction mixture was cooled to room temperature and the contents were eluted through a silica gel plug with ~ 10 mL of hexanes to remove the catalyst. Product **35** was eluted with CH_2Cl_2 . The filtrate was then pumped under vacuum to remove the volatiles.

Preparative Scale Procedure. In the glovebox, Cp^*ZrBn_3 (220 mg, 0.44 mmol) was added to an oven-dried, 20 mL J. Young-vial glass storage tube with a stir bar and dissolved in 10 mL of toluene. The tube was then sealed and placed on a high-vacuum line where 1-pentanethiol (1.0 mL, 8.1 mmol) and 1-hexyne (2.5 mL, 22 mmol)²⁴ were syringed into the tube under an argon flush. The vessel was next sealed and placed in a preheated 100 °C oil bath for 24 h. After cooling, the vessel was opened to ambient and the catalyst was removed by filtering through silica gel, eluting with ~ 20 mL of hexanes. The volatiles were then removed under vacuum to yield pure **12** as a yellow oil (1.08 g, 5.8 mmol, 72% yield) which was determined to be 99% Markovnikov pure by GC/MS.

Phenylacetylene-*d* (30-*d*). In an oven-dried, 200 mL Schlenk flask, phenylacetylene (7.0 mL, 64 mmol) was dissolved in 60 mL of anhydrous diethylether. The flask was cooled to 0 °C before the slow addition of 45 mL of $^n\text{BuLi}$ solution (1.6 M in hexanes, 72 mmol) and stirring for 15 min at 0 °C, followed by 30 min at room temperature. The flask was recooled to 0 °C, and D_2O (2.5 mL, 125 mmol) was slowly added. The reaction was stirred overnight at room temperature before the solvent was removed in vacuo, and the product was distilled to afford a clear liquid in 57% yield. The deuterium incorporation was determined to be 98% atom % D by ^1H NMR. ^1H NMR (benzene- d_6 , 500 MHz, δ): δ 7.40 (m, 2H); 6.91 (m, 3H). ^{13}C NMR (benzene- d_6 , 125 MHz, δ): δ 132.7; 129.1; 128.9; 123.1; 83.8 (t, 7.5 Hz); 78.0 (t, 38 Hz). ^2H (benzene- d_6 , 61 MHz, δ): δ 2.68 (s).

Ethanethiol-*d* (7-*d*). ^1H NMR (benzene- d_6 , 500 MHz, δ): δ 2.16 (m, 2H); 0.97 (t, 7.0 Hz, 1H). ^{13}C NMR (benzene- d_6 , 125 MHz, δ): δ 20.1; 19.3. ^2H (benzene- d_6 , 61 MHz, δ): δ 1.07 (s).

2-(Ethylthio)-1-hexene (8). ^1H NMR (benzene- d_6 , 500 MHz, δ): δ 5.01 (s, 1H); 4.66 (s, 1H); 2.43 (q, 7.5 Hz, 2H); 2.22 (t, 7.5 Hz, 2H); 1.55 (m, 2H); 1.24 (m, 2H); 1.06 (t, 7.5 Hz, 3H); 0.83 (t, 7.5 Hz, 3H). ^{13}C NMR (benzene- d_6 , 125 MHz, δ): δ 146.8; 105.2; 38.1; 31.8; 25.6; 22.7; 14.4; 13.7. HRMS (EI) m/z calcd for $\text{C}_8\text{H}_{16}\text{S}$: 144.0973; found: 144.0966.

2-(2,2,2-Trifluoroethylthio)-1-hexene (10). ^1H NMR (benzene- d_6 , 400 MHz, δ): δ 4.90 (s, 1H); 4.75 (s, 1H); 2.69 (q, 10 Hz, 2H); 2.00 (t, 7.6 Hz, 2H); 1.34 (m, 2H); 1.40–1.30 (m, 2H); 1.17–1.07 (m, 2H); 0.78 (t, 7.2 Hz, 3H). ^{13}C NMR (benzene- d_6 , 100 MHz, δ): δ 143.5; 129.0; 110.2; 36.9; 33.8 (q, $J_{\text{FC}} = 10$ Hz); 31.0; 22.5; 14.3. HRMS (EI) m/z calcd for $\text{C}_8\text{H}_{13}\text{F}_3\text{S}$: 198.0690; found: 198.0684.

2-(Phenylmethylthio)-1-hexene (17). ^1H NMR (benzene- d_6 , 500 MHz, δ): δ 7.22 (d, 7.5 Hz, 2H); 7.08 (t, 8.0 Hz, 2H); 7.01 (t, 7.5, 1H); 4.98 (s, 1H); 4.73 (s, 1H); 3.69 (s, 2H); 2.19 (t, 7.5 Hz, 2H); 1.51 (m, 2H); 1.22 (m, 2H); 0.81 (t, 7.5, 3H). ^{13}C NMR (benzene- d_6 , 125 MHz, δ): δ 147.0; 137.6; 129.5; 129.0; 127.6; 106.3; 37.9; 36.8; 31.7; 22.7; 14.4. HRMS (EI) m/z calcd for $\text{C}_{13}\text{H}_{18}\text{S}$: 206.1129; found: 206.1127.

3-Cyclohexyl-2-(pentylthio)-1-propene (25). ^1H NMR (benzene- d_6 , 500 MHz, δ): δ 5.02 (s, 1H); 4.74 (s, 1H); 2.53 (t, 7.0 Hz, 2H); 2.18 (d, 7.0 Hz, 2H); 1.83–1.78 (m, 2H); 1.78–1.70 (m, 1H); 1.70–1.63 (m, 2H); 1.63–1.56 (m, 1H); 1.56–1.48 (m, 2H); 1.26–1.04 (m, 7H); 0.87–0.78 (m, 5H). ^{13}C NMR (benzene- d_6 , 125 MHz, δ): δ 145.5; 106.0; 46.7; 37.3; 33.6; 31.9; 31.7; 28.6; 27.3; 27.0; 22.9; 14.5. HRMS (EI) m/z calcd for $\text{C}_{14}\text{H}_{26}\text{S}$: 226.1755; found: 226.1748.

2-(Pentylthio)-3-phenyl-1-propene (27). ^1H NMR (benzene- d_6 , 500 MHz, δ): δ 7.20–7.16 (m, 2H); 7.15–7.10 (m, 2H); 7.06–7.01 (m, 1H); 4.96 (s, 1H); 4.73 (s, 1H); 3.44 (s, 2H); 2.42 (t, 7.5 Hz, 2H); 1.44–1.36 (m, 2H); 1.13–1.01 (m, 4H); 0.72 (t, 7.0 Hz, 3H). ^{13}C NMR (benzene- d_6 , 125 MHz, δ): δ 146.4; 139.5; 129.7; 128.9; 127.1; 107.1; 44.5; 31.9; 31.8; 28.5; 22.9; 14.4. HRMS (EI) m/z calcd for $\text{C}_{14}\text{H}_{20}\text{S}$: 220.1286; found: 220.1287.

3-(1-(Pentylthio)ethenyl)pyridine (33). ^1H NMR (benzene- d_6 , 500 MHz, δ): δ 9.05 (s, 1H); 8.46 (dd, 5.0 Hz, 1H); 7.59 (dt, 8.0 Hz, 1H); 6.66 (dd, 8.0 Hz, 1H); 5.24 (s, 1H); 5.04 (s, 1H); 2.37 (t, 7.5 Hz, 2H); 1.40 (m, 2H); 1.15–1.05 (m, 4H); 0.77 (t, 7.0 Hz, 3H). ^{13}C NMR (benzene- d_6 , 125 MHz, δ): δ 150.4; 149.2; 143.2; 136.1; 134.5; 123.4; 112.0; 32.5; 31.5; 28.7; 22.8; 14.4. HRMS (APPI) m/z $[\text{M}+\text{H}]^+$ calcd for $\text{C}_{12}\text{H}_{17}\text{NS}$: 208.1161; found: 208.1158.

2-(Pentylthio)-2-propen-1-amine (35). ^1H NMR (benzene- d_6 , 500 MHz, δ): δ 5.16 (s, 1H); 4.74 (s, 1H); 3.26 (s, 2H); 2.49 (t, 7.5 Hz, 2H); 1.49 (m, 2H); 1.26–1.06 (m, 4H); 0.87–0.63 (bm, 5H). ^{13}C NMR (benzene- d_6 , 125 MHz, δ): δ 149.5; 105.1; 48.8; 31.8; 31.5; 28.8; 22.9; 14.5. HRMS (ESI) m/z $[\text{M}+\text{H}]^+$ calcd for $\text{C}_8\text{H}_{18}\text{NS}$: 160.1154; found: 160.1155.

Results

The principal goal of this investigation is to explore the efficacy and scope of organozirconium complexes in terminal alkyne hydrothiolation processes and to elucidate the mechanism by which this transformation occurs. Ancillary ligand effects on catalyst stability and reactivity are first discussed, accompanied by a presentation of substrate scope, followed by substrate steric and electronic effects on hydrothiolation activity and selectivity. Finally, reaction kinetics and deuterium labeling studies are presented, including rate law and activation parameters, and their implications regarding a proposed mechanistic pathway are discussed.

Ligand Effects on Catalyst Stability and Reactivity. With the hydrothiolation of 1-hexyne as a model reaction, the catalytic activity of a variety of organozirconium complexes was examined by *in situ* ^1H NMR spectroscopy for efficiency in this transformation. It is found that catalyst activity, stability,

(23) (a) Anslyn, E. V.; Dougherty, D. A. *Modern Physical Organic Chemistry*; University Science Books: Sausalito, CA, 2006. (b) Espenson, J. H. *Chemical Kinetics and Reaction Mechanisms*, 2nd ed.; McGraw-Hill: New York, 1995. (c) Pilling, M. J.; Seakins, P. W. *Reaction Kinetics*; Oxford University Press: New York, 1995.

(24) Because this reaction is first-order in thiol and alkyne, excess alkyne is necessary to drive the reaction to near completion. NMR scale reactions of **6** + **11** \rightarrow **12** mediated by complex **2** at 120 °C results in 50% conversion after 24 h with 2 \times excess alkyne while resulting in 95% conversion with 3 \times excess alkyne.

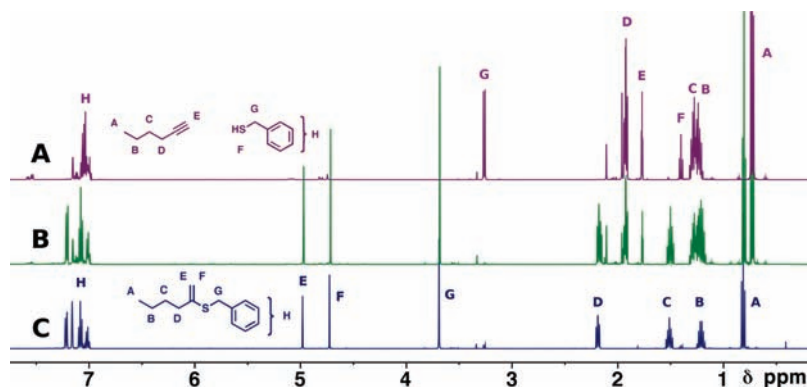


Figure 1. ^1H NMR (500 MHz) of reaction $6 + 16 \rightarrow 17$ mediated by 5 mol % Cp^*ZrBn_3 (**2**) precatalyst in benzene- d_6 with $3\times$ molar excess of 1-hexyne (A), the completed reaction after 24.0 h in a 120°C oil bath (B), and the isolated product (C, **17**).

Table 1. Turnover Frequencies for the Catalytic Zirconium-Mediated Hydrothiolation of 1-Hexyne (**6**) by Benzylmercaptan (**16**) and 1-Pentanethiol (**11**)

Precatalyst	Benzylmercaptan N_t (h^{-1})	1-Pentanethiol N_t (h^{-1})
1 , CGCZrMe_2	3.0	0.7
2 , Cp^*ZrBn_3	1.5	1.5
3 , $\text{Cp}^*\text{ZrCl}_2\text{NMe}_2$	5.9 ^a	--
4 , $\text{Cp}^*_2\text{ZrMe}_2$	--	low activity
5 , $\text{Zr}(\text{NMe}_2)_4$	≥ 2.0 ^b	--

^a Catalyst structure changes are observed during the reaction likely as a result of known chloride redistribution.³⁰ ^b Exact turnover-frequency (N_t) cannot be determined due to the catalyst precipitation after addition of benzylmercaptan (**16**).

and selectivity are strongly dependent on the nature of the zirconium ancillary ligation (a representative experiment is shown in Figure 1). Thus, addition of $20\times$ excess thiol to tetrakis(dimethylamido)zirconium(IV) (**5**) results in rapid precipitation of a new complex which will be discussed in more detail below. However, precipitation is not observed for cyclopentadienyl catalysts **1–4** except when $[\text{thiol}] \geq 1.2\text{ M}$. In contrast to reports of excess thiol protonolytically cleaving the cyclopentadienyl ligands of organoactinide and organolanthanide cyclopentadienyl complexes with subsequent precipitation of aggregated thiolate species,^{11,25} ring cleavage is not observed²⁶ under the present conditions (as assessed by *in situ* NMR spectroscopy), consistent with more covalent Zr–Cp bonding.²⁷

For the hydrothiolations surveyed, the measured turnover frequencies (Table 1) are dependent upon the particular zirconium ancillary ligation and thiol reagent. In the reaction between 1-hexyne (**6**) and 1-pentanethiol (**11**), Cp^*ZrBn_3 (**2**, $\text{Cp}^* = \text{C}_5\text{Me}_5$, $\text{Bn} = \text{benzyl}$) is more than $2\times$ as active as CGCZrMe_2 (**1**, $\text{CGC} = \text{Me}_2\text{SiCp}''\text{NCMe}_3$, $\text{Cp}'' = \text{C}_5\text{Me}_4$) followed by

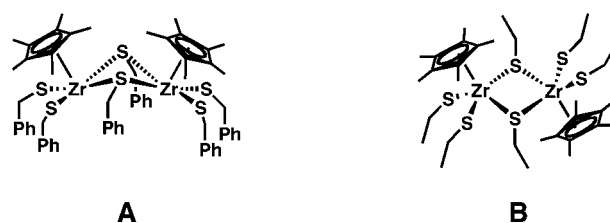


Figure 2. Zirconium thiolate dimers with μ -bridging thiolates resulting from the reaction of Cp^*ZrBn_3 (**20**) with either benzylmercaptan (**16**) or ethanethiol (**7**) to yield known cisoid benzylate (A) and transoid ethanethiolate (B) dimers.³¹

$\text{Cp}^*_2\text{ZrMe}_2$ (**4**), which is activated very slowly (i.e., undergoes slow Zr–Me cleavage)²⁸ and exhibits very low net activity. In contrast, changing to benzylmercaptan (**16**) evidences a reverse order of activity with CGCZrMe_2 (**1**) exhibiting $2\times$ the activity of Cp^*ZrBn_3 . Tetrakis(dimethylamido)zirconium(IV) (**5**) exhibits higher initial reactivity than Cp^*ZrBn_3 (**2**) with benzylmercaptan (**16**); however, gradual precipitation of zirconium-containing side products renders the exact turnover frequency undeterminable.²⁹

Nature of the Catalytic Species. To test for oligomeric species such as the known dimers of the formula $[\text{Cp}^*\text{Zr}(\text{SR})_3]_2$ ³¹ (Figure 2) under the present hydrothiolation conditions, a Teflon-valved NMR tube was loaded with Cp^*ZrBn_3 (**1**) and a 20-fold excess of both benzylmercaptan (**16**) and 1-hexyne (**6**). The resulting ^1H NMR spectrum (Figure 3A) of the known cisoid $[\text{Cp}^*\text{Zr}(\text{SBN})_3]_2$ dimer (Figure 2A) at 23°C is observed with spectral parameters in good agreement with reported literature NMR data.³¹ Upon heating the solution to 120°C (Figure 3B), the terminal benzylthiolate methylene protons at δ 5.11 and 4.82 ppm broaden and shift upfield to δ 4.96 and 4.73 ppm, respectively, resulting in the latter resonance overlapping with the bridging methylene resonance (Figure 3b). When the reaction mixture is cooled to 60°C (Figure 3C) and subsequently to 23°C (Figure 3D), the methylene resonances sharpen, separate, and return to their original frequencies. Exchange between

(25) (a) Cotton, S. *Lanthanide and Actinide Chemistry*; John Wiley & Sons, Ltd: Uppington, Rutland, U.K., 2006. (b) Li, H. X.; Ren, Z. G.; Zhang, Y.; Zhang, W. H.; Lang, J. P.; Shen, Q. *J. Am. Chem. Soc.* **2005**, *127*, 1122–1123. (c) Aspinall, H. C., *Chemistry of the f-Block Elements*; Taylor & Francis: Washington, DC, 2001. (d) Aspinall, H. C.; Cunningham, S. A.; Maestro, P.; Macaudiere, P. *Inorg. Chem.* **1998**, *37*, 5396–5398. (e) Marks, T. J. *Science*, **1982**, *217*, 989–997.

(26) Even at $[\text{thiol}] > 1.2\text{ M}$, when small amounts of precipitate are formed, no free CGCH_2 ligand is observed by NMR spectroscopy.

(27) Strittmatter, R. J.; Bursten, B. E. *J. Am. Chem. Soc.* **1991**, *113*, 552–559.

(28) Activation in 120°C occurs slowly and thus sometimes requires placing the reaction in a 140°C oil bath overnight for complete activation.

(29) A rate for 1-pentanethiol (**11**) with $\text{Zr}(\text{NMe}_2)_4$ (**5**) is not obtainable due to an immediate precipitation of deep blue complex. The mixture of $\text{Zr}(\text{NMe}_2)_4$ (**5**) and benzylmercaptan (**16**) more slowly produces a bright orange precipitate under identical conditions.

(30) Erker, G.; Froemberg, W.; Benn, R.; Mynott, R.; Angermund, K.; Krueger, C. *Organometallics* **1989**, *8*, 911–920.

(31) Heyn, R. H.; Stephan, D. W. *Inorg. Chem.* **1995**, *34*, 2804–2812.

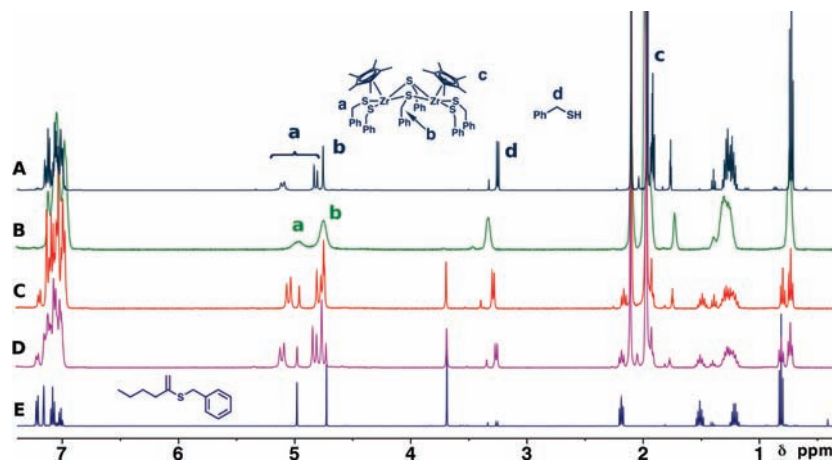
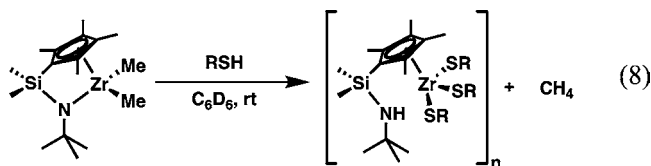


Figure 3. ^1H NMR spectra in benzene- d_6 of the dimer formed from reaction of benzylmercaptan (**16**) and Cp^*ZrBn_3 (**2**) during hydrothiolation of 1-hexyne (**6**). Initial ^1H NMR spectrum (500 MHz) of starting materials at 23 °C (A), ^1H NMR spectrum (400 MHz) of reaction mixture at 120 °C with broadening of signals of a and b (B), ^1H NMR spectrum (400 MHz) after cooling to 60 °C (C), ^1H NMR spectrum (400 MHz) after cooling to 23 °C (D), and the isolated product (**17**, E).

bridging and terminal benzylthiolate ligands³² (Figure 3a,b) along with free thiol (Figure 3d) is also verified by 1D NOESY NMR spectroscopy. The known transoid $[\text{Cp}^*\text{Zr}(\text{SEt})_3]_2$ dimer³¹ (Figure 2B) with bridging ethanethiolates is also observed in these studies by addition of ethanethiol to Cp^*ZrBn_3 (**2**). The NMR data are in good agreement with literature values.³¹ Based on the *in situ* observation of a N–H resonance in the ^1H NMR spectra of complex **1**, the 3:1 ^1H NMR integration of thiolate to CGC ligands, and the known ability of thiols to displace amide ligands from Zr(IV) complexes,³³ we suggest that coordination of the CGC ligand is predominantly Cp-only in the presence of excess thiol (eq 8).



Thiol Effects on Hydrothiolation Rates. Using CGCZrMe_2 (**1**) as a representative precatalyst, a diverse group of thiols offering variations in steric, electronic, and bonding energetic characteristics was investigated in 1-hexyne (**6**) hydrothiolation. Results are summarized in Table 2 and show that steric encumbrance is a major factor in determining the reaction turnover frequency, with bulkier thiols exhibiting severely retarded activity. In transitioning from a primary to a secondary thiol (Table 2, entry 3 \rightarrow 4), a greater than 50 \times rate reduction is observed. No reactivity is observed with a tertiary thiol (Table 2, entry 5), presumably due to the increased nonbonding repulsions. A comparison of primary thiol chain length effects reveals a slight reduction in rate for 1-pentanethiol (**11**) \rightarrow ethanethiol (**7**) (Table 2, entries 1 and 3). Aromatic thiol functionality also influences 1-hexyne (**6**) hydrothiolation rates with the introduction of thiol phenyl groups markedly enhancing the turnover frequencies. Thus, transitioning from cyclohexylmercaptan (**13**) to thiophenol (**18**) (Table 2, entries 4 and 7) results in a 20 \times increase in rate, while the turnover frequencies of 1-pentanethiol (**11**) versus benzylmercaptan (**16**) (Table 2,

entries 3 and 6) evidence a 5 \times increase in rate, despite increased steric encumbrance. To assay electronic effects on the rates, turnover frequencies of ethanethiol (**7**) and 2,2,2-trifluoroethanethiol (**9**)³⁴ were also measured and reveal no significant fluorocarbon effects (Table 2, entries 1, 2).

Alkyne Effects on Hydrothiolation Rates. Alkyne structure also affects the rate of hydrothiolation; however steric encumbrance exhibits a less pronounced influence than electronic characteristics. Switching from an α -monosubstituted to an α -disubstituted alkyne results in a moderate decrease in rate (Table 2, entry 1 and Table 3, entry 1 respectively). Product formation with an α -trisubstituted alkyne (Table 3, entry 2) is observed by ^1H NMR and GC/MS, although the yield is very low. Similar to the aforementioned trend with thiols, alkyne electronic characteristics also play a prominent role in influencing hydrothiolation rates, with conjugated alkynes exhibiting significantly enhanced rates. In particular, introduction of unsaturation α to the $\text{C}\equiv\text{C}$ bond results in a 5 \times rate increase versus the unconjugated alkyne (Table 3, entries 1 and 5) while phenylacetylene (**30**) increases the activity 4 \times versus the cyclohexylacetylene (**20**) (Table 3, entries 1 and 6). Rate enhancement is also observed with a 3-ethynylpyridine (**32**) (Table 3, entry 7), although not as pronounced as that for phenyl substitution (Table 3, entry 6).

Reactivity and Selectivity Trends with Propargylamine. The incorporation of an aliphatic amine functionality into the alkyne substrate results in a dramatic hydrothiolation rate enhancement with the degree of Markovnikov selectivity strongly dependent on the structure of the precatalyst (Table 4). For propargylamine (**34**), the substrate turnover frequency increases 3 \times and 7 \times with Cp^*ZrBn_3 (**2**) and CGCZrMe_2 (**1**) as precatalysts, respectively, versus the corresponding 1-hexyne (**6**) hydrothiolation. While Cp^*ZrBn_3 (**2**) yields the Markovnikov product (**35**) with 98% selectivity (Table 4, entry 2), CGCZrMe_2 (**1**) results in only 75% Markovnikov selectivity (Table 4, entry 2). The addition of radical inhibitor γ -terpinene^{51,11} with CGCZrMe_2 (**1**) affords no significant change in selectivity (Table 4, entry 3).³⁵

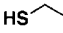
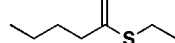
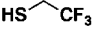
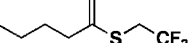

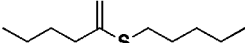
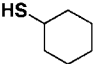
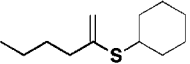
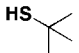
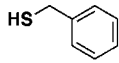
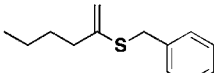
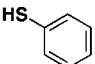
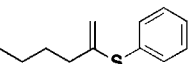
(32) Fritzing, B.; Moreels, I.; Lommens, P.; Koole, R.; Hens, Z.; Martins, J. C. *J. Am. Chem. Soc.* **2009**, *131*, 3024–3032.

(33) Chandra, G.; Lappert, M. F. *J. Chem. Soc. A* **1968**, 1940–1945.

(34) (a) Gregory, M. J.; Bruce, T. C. *J. Am. Chem. Soc.* **1960**, *89*, 2121–2127. (b) Danehy, J. P.; Noel, C. J. *J. Am. Chem. Soc.* **1960**, *82*, 2511–2515.

(35) Additionally, 3-buten-1-ol was tested together with 1-pentanethiol (**11**) and compound **1**. No hydrothiolation activity was observed.

Table 2. Catalytic Organozirconium-Mediated Intermolecular Hydrothiolation of 1-Hexyne (6)

Entry	Thiol	Product	Selectivity(%) ^a with (2)	Conversion(%) ^b with (2)	N _t (h ⁻¹) ^c with (1)
1.	 7	 8	96	95	0.6
2.	 9	 10	84	79	0.6
3.	 11	 12	94	95	0.7
4.	 13	 14	59 ^d	7 (55) ^d	0.008
5.	 15	--	--	--	N.R.
6.	 16	 17	95	95	3.0
7.	 18	 19	94	94	0.2

^a Markovnikov selectivity determined by ¹H NMR and CG/MS after 24.0 h in a 120 °C oil bath with 5 mol % **2** and a 3× molar excess of alkyne.

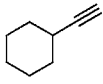
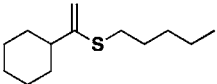
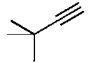
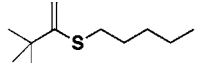
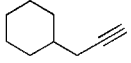
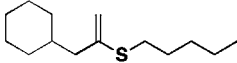
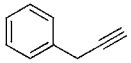
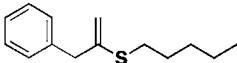
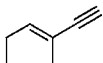
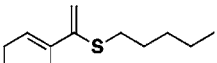
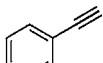
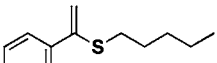
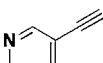
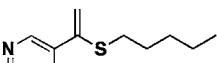
^b Yield determined by ¹H NMR with respect to thiol after 24.0 h in a 120 °C oil bath with 5 mol % **2** and a 3× excess of alkyne. ^c Turnover frequencies measured in a 120 °C oil bath with 5 mol % **1** with a 1:1 alkyne:thiol ratio. ^d After 7 days in a 120 °C oil bath.

Radical Side Reactions. The observation of anti-Markovnikov product isomers is reasonably attributed to a known, radical side reaction⁴ (eq 1a) competing with the insertive/protonolytic catalytic mechanism (see Discussion below). By adding the radical inhibitor γ -terpinene,^{5i,11} the Markovnikov selectivity of the reaction **6** + **11** \rightarrow **12** mediated by 1 mol % **1** is increased from 4:1 to 50:1 as assayed by ¹H NMR and GC/MS. Further, by increasing the catalyst concentration (Figure 4), Markovnikov selectivity is further enhanced up to 99% (Figure 4). However, neither high catalyst loadings nor radical inhibitor completely eliminates the anti-Markovnikov products, indicating that some may be due to imperfect, intrinsic catalytic selectivity.

Kinetic and Mechanistic Studies of Organozirconium-Mediated Alkyne Hydrothiolation. Kinetic studies were performed to define the hydrothiolation reaction pathway and to better understand the influence of [catalyst], [thiol], and [alkyne] on

the sequence of reaction events. Experiments were conducted on the CGCZrMe₂ (**1**)-mediated hydrothiolation of 1-hexyne (**6**) by 1-pentanethiol (**11**), and kinetic results are plotted in Figure 5. The empirical rate law is derived by systematically varying the concentration of CGCZrMe₂ (**1**), 1-pentanethiol (**11**), and 1-hexyne (**6**) at 120 °C. Experiments carried out by varying [CGCZrMe₂ (**1**)] over the range 1.9–21 mM exhibit a clear, linear trend when plotted against the measured rate (Figure 5B) indicating a first-order dependence of rate on catalyst concentration. By varying [1-hexyne (**6**)] over the range 0.1–0.5 M, a first-order trend is also observed in the plot of [1-hexyne (**6**)] versus product formation rate (Figure 5C). The varying of 1-pentanethiol (**11**) concentration reveals a more complex trend, with an approximate first-order behavior for [**11**] < 0.3 M, followed by saturation in the rate at concentrations > 0.3 M (Figure 5D). As a result, the empirical rate law for the reaction

Table 3. Catalytic Organozirconium-Mediated Intermolecular Alkyne Hydrothiolation by 1-Pentanethiol (**11**) as a Function of Alkyne

Entry	Alkyne	Product	Selectivity(%) ^a with (2)	Conversion(%) ^b with (2)	N _t (h ⁻¹) ^c with (1)
1.	 20	 21	92	92	0.4
2.	 22	 23	--	--	-- ^d
3.	 24	 25	96	98	0.3
4.	 26	 27	91	Quant. ^e	1.5
5.	 28	 29	75 (97) ^f	Quant. ^e	2.2
6.	 30	 31	66	Quant. ^e	1.6
7.	 32	 33	90	Quant. ^e	1.2

^a Markovnikov selectivity determined by ¹H NMR and CG/MS after 24.0 h at 120 °C with 5 mol % **2** and a 3× excess of alkyne. ^b Yield determined by ¹H NMR with respect to thiol after 24.0 h in 120 °C with 5 mol % **2** and a 3× molar excess of alkyne. ^c Turnover frequencies measured in a 120 °C oil bath with 5 mol % **1** with a 1:1 alkyne:thiol ratio. ^d Hydrothiolation activity observed by ¹H NMR and confirmed through GC/MS, although the yield is very low. ^e Quantitative by ¹H NMR with respect to thiol. ^f With the addition of γ -terpinene radical inhibitor in a 1:1 molar ratio to alkyne.

6 + **11** → **12** is described by eq 9 with [CGCZrMe₂ (**1**)] and [1-hexyne (**6**)] both first-order, and [1-pentanethiol (**11**)] *x*-order with *x* = 1 for [1-pentanethiol (**11**)] ≤ 0.3 M and *x* = 0 for [1-pentanethiol (**11**)] ≥ 0.3 M. Additional catalyst- and alkyne-dependence studies performed under high [thiol] conditions (i.e., [thiol] = 1.2 M) show that [alkyne] and [catalyst] remain first-order even at elevated [thiol].

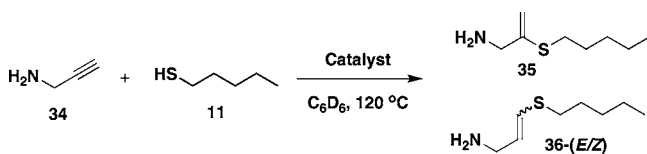
$$\text{Rate} = k_{\text{obs}}[\text{CGCZr}]^1[\text{1-hexyne}]^1[\text{1-pentanethiol}]^x \quad (9)$$

To derive activation parameters, the rate of the conversion **6** + **11** → **12** mediated by **1** was analyzed from 50 to 80 °C,

and the data were plotted with respect to the Eyring equation. Variable temperature studies at 0.2 M [alkyne] and [thiol] result in an Eyring plot yielding $\Delta H^\ddagger = +18.1(1.2)$ kcal/mol and $\Delta S^\ddagger = -20.9(2.5)$ e.u. Repeating the temperature studies with [thiol] = 1.2 M from 40 to 80 °C yields similar reaction parameters of $\Delta H^\ddagger = +17.8(1.5)$ kcal/mol and $\Delta S^\ddagger = -24.4(4.8)$ e.u.³⁶

To trace the fate of the D—C≡C—R' hydrogens in the present catalytic transformations, deuterium-labeling experiments were performed using deuterated phenylacetylene (**30-d**). Upon addition of 1-pentanethiol (**11**) and **30-d** to CGCZrMe₂ (**1**) at

Table 4. Catalytic Zirconocene-Mediated Intermolecular Hydrothiolation of Propargylamine (**34**) with 1-Penthanethiol (**11**) as a Function of Precatalyst



Entry	Precatalyst	Selectivity (%) for 35	N_t (h^{-1})	γ -Terpinene Addition ^a
1	2 , Cp*ZrBn ₃	98	4.8	No
2	1 , CGCZrMe ₂	75	4.7/3.3 ^b	No
3	1 , CGCZrMe ₂	76	--	Yes

^a Radical inhibitor was added in a 1:1 molar ratio to alkyne. ^b Initial turnover frequency for anti-Markovnikov products (**36-E/Z**).

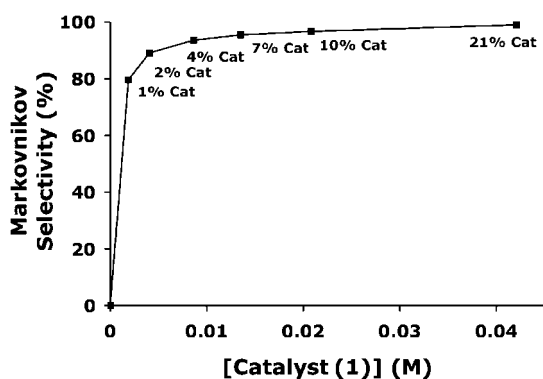
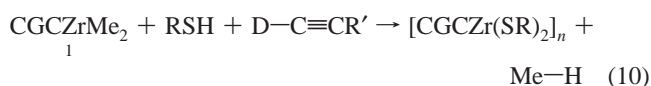


Figure 4. Plot of Markovnikov selectivity versus CGCZrMe₂ (**1**) precatalyst concentration for the transformation **6** + **11** → **12** (thiol:alkyne = 1:1). Data points show mol % catalyst versus substrate at fixed substrate concentration.

room temperature, a single methane (CH₄) resonance³⁷ is immediately observed in the ¹H NMR spectrum (eq 10).



The absence of CH₃-D³⁸ suggests exclusive activation of the catalyst by thiol protonolysis despite known alkyne protonolysis activity.³⁹ To further rule out alkyne-mediated protonolysis as a kinetically significant route for the cleavage of Zr–alkyl bonds, relative rates of alkyne- and thiol-mediated protonolysis were examined in the activation of Cp*₂ZrMe₂ (**4**). By addition of either 1-hexyne (**6**) or 1-penthanethiol (**11**) to **4**, thiol protonolysis of the Zr–Me bonds is measured to be 150× more rapid than the analogous alkyne protonolysis.

An apparent KIE of $k_H/k_D = 1.3(0.1)$ is measured for the reaction **11** + **30-d** catalyzed by complex **1**, consistent with a

secondary kinetic isotope effect.⁴⁰ At early reaction times, a single olefinic resonance appears in the ¹H NMR at δ 5.13 ppm (Figure 6A) assigned to product **31-D_E** by 1D NOESY NMR. In addition, ²H NMR shows a single product deuterium resonance at δ 5.4 ppm. Upon further heating, additional product olefinic resonances appear in the ¹H NMR spectra at δ 5.41, 5.40, and 5.14 ppm (Figure 6B–D) with a second olefinic resonance in the ²H NMR at δ 5.1 ppm indicating the formation of products **31**, **31-D_Z**, and possibly **31-D₂**.⁴¹ Interestingly, a deuterium resonance is also observed growing in at δ 1.07 ppm indicating deuteration of the thiol (i.e., RSD).^{42,43} To further examine the deuterium exchange from alkyne-*d* to thiol, phenylacetylene-*d* (**30-d**), *tert*-butylmercaptan (**15**), and **1** were dissolved in benzene-*d*₆ and heated at 120 °C for 9 h. Despite no evidence of zirconium-mediated hydrothiolation, deuterium/proton exchange is observed by ¹H and ²H NMR spectroscopy, indicating that the exchange is independent of the zirconium-mediated hydrothiolation pathway. A similar combination of **30-d** and **11** without catalyst evidences no deuterium exchange showing that zirconium is involved in the isotopic exchange process.

Discussion

Catalyst Ancillary Ligand Effects on Activity for Intermolecular Terminal Alkyne Hydrothiolation. The choice of cyclopentadienyl and other ligands has a critical effect on Zr-mediated hydrothiolation activity. The high activity observed with the Cp*ZrCl₂NMe₂ (**3**) precatalyst is consistent with reported organozirconium-mediated hydroamination rate enhancement by chloride ligands.^{17b} Given the large influence of thiol steric characteristics on insertion kinetics, this possibly reflects decongestion of the metal center, with the chlorides offering less steric encumbrance around the metal center versus thiolates. Conversely, the slow activation and hydrothiolation by Cp*₂ZrMe₂ (**4**) appears to be a result of severe, nonbonded repulsions incurred by the bis(pentamethylcyclopentadienyl) ligation. Because of the predominantly Cp-based bonding of the CGC ligand, differences in rate between CGCZrMe₂ (**1**) and Cp*ZrBn₃ (**2**) are likely the result of optimal sterics or polar interactions with the CGC amine functionality (see below).

Nature of Catalytic Species. Zirconium ancillary ligation exerts dramatic effects on catalyst stability. First, the presence of a cyclopentadienyl-based ligand avoids suspected, detrimental catalyst aggregation^{31,44} and subsequent precipitation from solution following the addition of excess thiol to the precatalyst. Since no olefinic resonances are observed which would indicate thiol C–S bond cleavage by the metal, as was reported by Kanatzidis and co-workers,⁴⁴ the precipitation is believed to be the result of catalyst aggregation yielding insoluble thiolate species.⁴⁵ While mono-Cp* zirconium species are known in the literature to undergo dimerization,³² Cp*₂Zr(SR)₂ species remain monomeric.⁴⁶ Therefore, the Cp-based ligands likely provide steric protection from oligomerization to higher molecular weight, insoluble species.

(36) For thermodynamic estimates, Eyring and Arrhenius plots, and kinetic data at [Thiol] = 1.2 M, see Supporting Information.

(37) Williams, L. A.; Marks, T. J. *Organometallics* **2009**, *28*, 2053–2061.

(38) Assayed by ²H and ¹H NMR. The present study finds that CH₃D gives a triplet at 0.14 ppm in the ¹H NMR.

(39) (a) Roering, A. J.; Maddox, A. F.; Elrod, L. T.; Chan, S. M.; Ghebreab, M. B.; Donovan, K. L.; Davidson, J. J.; Hughes, R. P.; Shalumova, T.; MacMillan, S. N.; Tanski, J. M.; Waterman, R. *Organometallics* **2009**, *28*, 573–581. (b) Hoyt, H. M.; Bergman, R. G. *Angew. Chem., Int. Ed.* **2007**, *46*, 5580–5582. (c) Nishiura, M.; Hou, Z. *J. Mol. Catal. A: Chem.* **2004**, *213*, 101–106. (d) Wang, J.; Kapon, M.; Berthet, J. C.; Ephritikhine, M.; Eisen, M. S. *Inorg. Chim. Acta* **2002**, *334*, 183–192. (e) Dash, A. K.; Wang, J. Q.; Eisen, M. S. *Organometallics* **1999**, *18*, 4724–4741.

(40) Tobisu, M.; Nakai, H.; Chatani, N. *J. Org. Chem.* **2009**, *74*, 5471–5475.

(41) In addition to NMR, the formation of **31** and **31-D_{E/Z}** are also confirmed by HRMS. We are unable to support the formation of **31-D₂** by HRMS due to an overlapping ¹³C isotopic pattern.

(42) Stereochemical assignment of product vinyl proton resonances were determined by 1D NOESY NMR spectroscopy. For 1D NOESY NMR and ²H NMR spectra, see Supporting Information.

(43) Injecting ethanethiol-*d* (**7-d**) into a completed reaction did not result in deuterium incorporation into an already formed product.

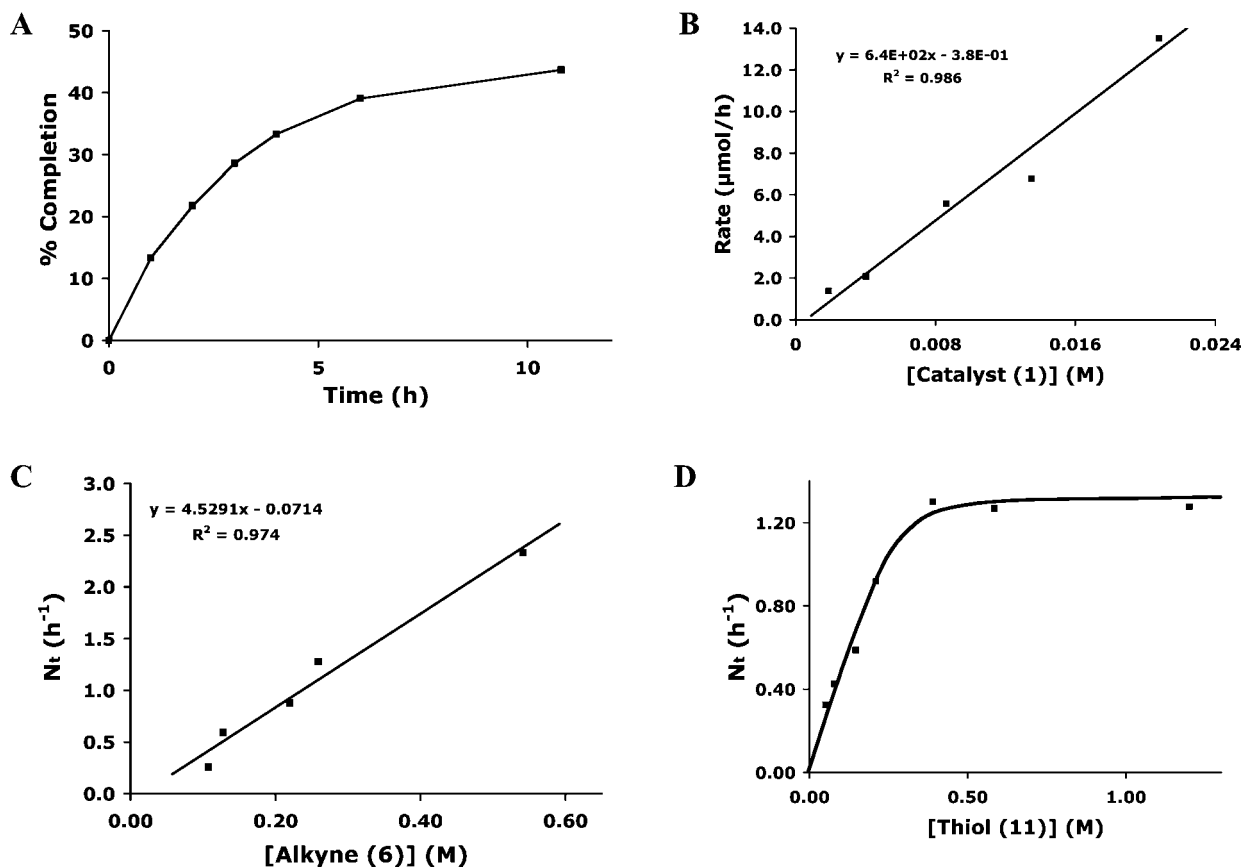


Figure 5. A representative plot of product formation rate against time for CGCZrMe₂ (1)-mediated hydrothiolation **6** + **11** → **12** (A). Plot of product formation rate of **6** + **11** → **12** versus [CGCZrMe₂ (1)] (B), [1-hexyne (6)] (C), and [1-pentanethiol (11)] (D) at [6] and [11] = 0.2 M unless otherwise indicated. All exhibit a first-order rate dependence on [catalyst] and [alkyne] at all explored concentrations and in [thiol] < 0.3 M. At [1-pentanethiol (11)] > 0.3 M, the [thiol] dependence shifts to zero-order. The lines in plots A, B, and C are least-squares fits, whereas the line in D is a numerically fit to eq S4 with $k_1 = 7 \text{ h}^{-1} \text{ M}^{-1}$, $k_{-1} = \text{h}^{-1}$, and $k_2 = 20 \text{ h}^{-1} \text{ M}^{-1}$.

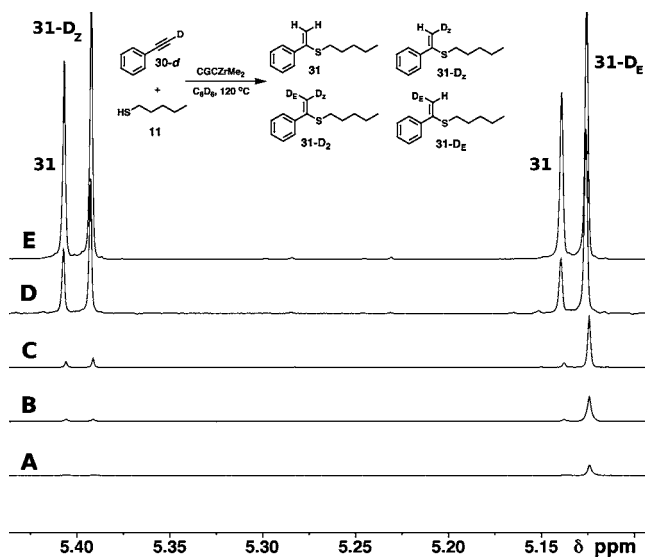


Figure 6. Hydrothiolation of **11** and **30-d** yields multiple isotopomers with deuterium incorporated in both the product *E* and *Z* positions. The ¹H NMR (500 MHz) spectrum in benzene-*d*₆ evidences product **31-DE** (5.13 ppm) after 0.20 h in a 120 °C oil bath (A). Additional **31** (5.41/5.14 ppm) and **31-D_Z** (5.40 ppm) resonances are observed after heating for 0.50 h (B), 1.00 h (C), 7.66 h (D), and 40.2 h (E). Signal strengths are normalized to an internal integration standard.

Given the tendency of zirconium-thiolates to undergo aggregation and that previously reported [Cp*Zr(μ -SR)(SR)₂]₂

zirconium-thiolate dimeric species are observed in the present reaction media,³² the catalyst resting state is reasonably suggested to be dimeric. Because the hydrothiolation rate is not half-order in [catalyst], it is unlikely that the zirconium-thiolates are involved in rapid dimer \rightleftharpoons monomer equilibration prior to entering the hydrothiolation cycle, as is the case for aggregated, hydrothiolation-active, Pd and Ni complexes.^{5h,i,1} This situation stands in contrast to reported Rh and Me₂SiCpTh hydrothiolation-active complexes which are proposed to be monomeric.^{5c,11,14a} DOSY⁴⁷ NMR experiments were performed on the [CGCZr(SR)₃]_n (R = pentyl, ethyl, and benzyl) species in an attempt to investigate the level of aggregation. However, due to the ambiguous nature of the ligand amine coordination to the zirconium center, reliable molecular volumes could not be calculated for comparison to the experimental results.⁴⁸ In the present complexes, exchange between bridging and terminal⁴⁹ thiolate ligands is also observed, along with evidence of protonolytic exchange between free thiol and bound thiolate ligands, indicating that the present zirconium-thiolate complexes are labile and stereochemically dynamic in solution.

(44) Coucouvanis, D.; Hadjikyriacou, A.; Lester, R.; Kanatzidis, M. G. *Inorg. Chem.* **1994**, *33*, 3645–3655.

(45) (a) Robertson, S. D.; Slawin, A. M. Z.; Woollins, J. D. *Polyhedron* **2006**, *25*, 823–826. (b) Friese, J. C.; Krol, A.; Puke, C.; Kirschbaum, K.; Giolando, D. M. *Inorg. Chem.* **2000**, *39*, 1496–1500. (c) Ashby, M. T.; Alguindigue, S. S.; Khan, M. A. *Inorg. Chem. Acta* **1998**, *270*, 227–237.

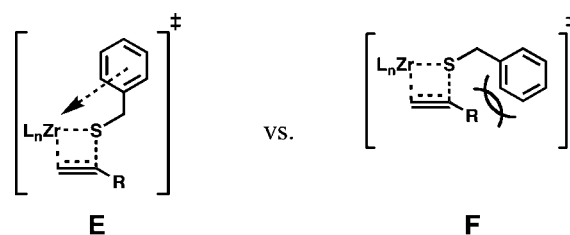
(46) Howard, W. A.; Trnka, T. M.; Parkin, G. *Inorg. Chem.* **1995**, *34*, 5900–5909.

Substrate Scope for Catalytic Intermolecular Terminal Alkyne Hydrothiolation. As can be seen from the data in Tables 2 and 3, cyclopentadienyl zirconium complexes are efficient precatalysts for transforming a wide range of thiols and terminal alkynes into vinyl sulfides with a high degree of Markovnikov selectivity. While many late-metal hydrothiolation catalysts can effect this transformation with arylthiols at varying levels of efficiency,^{2a,5c–o,8b} few are effective with less reactive aliphatic thiols.^{5c,d,i,m,50} In contrast, the present organozirconium complexes **1–4** are able to mediate hydrothiolation with aliphatic, benzylic, and aromatic thiols for the intermolecular, homogeneous hydrothiolation of a wide variety of terminal aliphatic, benzylic, and aromatic alkynes.

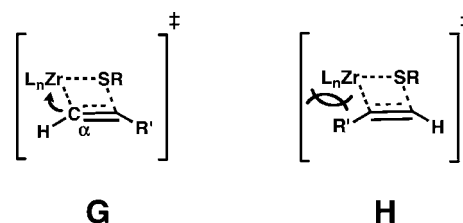
Thiol steric characteristics appear to be the dominant factor governing catalytic activity here, with secondary and tertiary thiols severely retarding hydrothiolation rates. This large rate dependence on nonbonded repulsions is consistent with multiple thiolate ligands^{45b,c,51} offering substantial steric congestion around the metal center as the alkyne insertion transition state is traversed. The thiol electronic characteristics also have a significant effect on the hydrothiolation turnover frequency, with the aromatic and benzylic thiols exhibiting the greatest activity. With no appreciable difference in rate between ethanethiol (**7**) and 2,2,2-trifluoroethanethiol (**9**), it can be concluded that alkyl electronic factors have less influence on catalytic turnover. Therefore, the rate enhancement observed as a result of the aromaticity is not likely due to electronic effects at the sulfur atom. One scenario invokes π -interaction of the arene with the electrophilic zirconium center.^{10g,52} This may lower the alkyne insertion barrier by π -electron stabilization of the electrophilic metal center^{8g,10g,53} (Scheme 2, **E**) or possibly reducing steric encumbrance at the metal center by restraining the thiol substituent (Scheme 2, **F**).

In contrast to thiols, alkyne steric factors have a lesser effect on the observed rates, with an α -monosubstituted alkyne exhibiting 1.5 \times the hydrothiolation rate of a similar α -disubstituted alkyne (Tables 2 and 3, entries 3 and 1, respectively). These observations are in agreement with turnover-limiting insertion of the alkyne into the Zr–SR bond where bulkier alkynes are expected to congest the metal coordination sphere in the turnover-limiting step to a lesser degree than analogous thiols. This likely reflects orientation of the alkyne substituent away from the bulky metal ligation (see below), with each

Scheme 2. A π -Interaction Drawing Away the Thiol Substituent (**E**) To Reduce Steric Interference during Alkyne Insertion (**F**) and Stabilize the Electrophilic Metal Center in the Insertive Transition State



Scheme 3. Proposed Insertive Transition States for the Formation of Markovnikov (**G**) and Anti-Markovnikov Hydrothiolation Products (**H**)



zirconium center coordinated to three thiolate ligands versus presumably only a single alkyne involved in the insertive transition state. Furthermore, alkyne substituent electronic characteristics significantly affect hydrothiolation activities with the effects more pronounced for alkynes than for thiols. As observed with late transition metal^{5c,l,m} and organothorium catalysts,¹¹ 3–5 \times rate increases are observed as a result of conjugation or aromaticity α to the C=C linkage (Table 3, **20** \rightarrow **28**, **30**, **32**), possibly the result of the π -system electron-withdrawing nature rendering the acetylene more electrophilic.

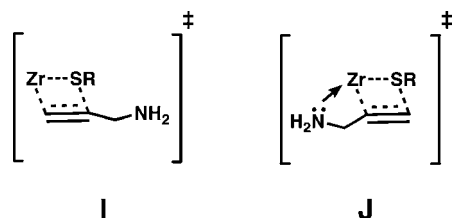
Regioselectivity of Intermolecular Terminal Alkyne Hydrothiolation. The present catalytic system is able to effect hydrothiolation processes with up to 99% Markovnikov selectivity and with no observable side products other than the occasional aforementioned anti-Markovnikov vinyl sulfides. An interplay of electronic and nonbonding repulsion in the four-membered insertive transition state is likely responsible for the high Markovnikov selectivity observed (Scheme 3). Reminiscent of lanthanide-mediated hydroamination,^{8g,53} the Markovnikov orientation of the acetylene with respect to the Zr–SR bond is expected to stabilize the electrophilic metal center in the transition state by placing greater electron density on the acetylene α carbon atom (Scheme 3, **G**). In addition, orientation of the R' substituent away from the bulky supporting ligation doubtlessly minimizes energetically unfavorable, nonbonding interactions (Scheme 3, **H**).

While anti-Markovnikov side products are occasionally observed in the present hydrothiolation reactions, they are not typically the result of organozirconium-centered catalytic reactions but rather arise from known, free radical side reactions.⁴ These competing processes can be suppressed by addition of

- (47) (a) Floquet, S. b.; Brun, S. b.; Lemonnier, J.-F.; Henry, M.; Delsuc, M.-A.; Prigent, Y.; Cadot, E.; Taulelle, F. *J. Am. Chem. Soc.* **2009**, *131*, 17254–17259. (b) Li, D.; Kagan, G.; Hopson, R.; Williard, P. G. *J. Am. Chem. Soc.* **2009**, *131*, 5627–5634. (c) Busetto, L.; Cassani, M. C.; Femoni, C.; Macchioni, A.; Mazzoni, R.; Zuccaccia, D. *J. Organomet. Chem.* **2008**, *693*, 2579–2591. (d) Bellachioma, G.; Ciancaleoni, G.; Zuccaccia, C.; Zuccaccia, D.; Macchioni, A. *Coord. Chem. Rev.* **2008**, *252*, 2224–2238. (e) Pianet, I.; André, Y.; Ducasse, M.-A. s.; Tarascou, I.; Lartigue, J.-C.; Pinaud, N. I.; Fouquet, E.; Dufour, E. J.; Laguerre, M. *Langmuir* **2008**, *24*, 11027–11035. (f) Macchioni, A.; Ciancaleoni, G.; Zuccaccia, C.; Zuccaccia, D. *Chem. Soc. Rev.* **2008**, *37*, 479–489.
- (48) (a) La-Scalea, M. A.; Menezes, G. M. S.; Ferreira, E. I. *THEOCHEM* **2005**, *730*, 111–120. (b) Zuccaccia, C.; Stahl, N. G.; Macchioni, A.; Chen, M.-C.; Roberts, J. A.; Marks, T. J. *J. Am. Chem. Soc.* **2004**, *126*, 1448–1464.
- (49) (a) Sirimanne, C. T.; Yu, Z.; Heeg, M. J.; Winter, C. H. *J. Organomet. Chem.* **2006**, *691*, 2517–2527. (b) Ashworth, N. J.; Conway, S. L. J.; Green, J. C.; Green, M. L. H. *J. Organomet. Chem.* **2000**, *609*, 83–88. (c) Thompson, R. L.; Lee, S.; Geib, S. J.; Cooper, N. J. *Inorg. Chem.* **1993**, *32*, 6067–6075.
- (50) This diminished activity has been attributed to the greater H–S bond enthalpies; see ref 5i.
- (51) Fandos, R.; Lanfranchi, M.; Otero, A.; Pellinghelli, M. A.; Ruiz, M. J.; Terreros, P. *Organometallics* **1996**, *15*, 4725–4730.

- (52) (a) Kissounko, D.; Epshteyn, A.; Fettinger, J. C.; Sita, L. R. *Organometallics* **2006**, *25*, 531–535. (b) O'Connor, P. E.; Morrison, D. J.; Steeves, S.; Burrage, K.; Berg, D. J. *Organometallics* **2001**, *20*, 1153–1160. (c) Bouwkamp, M.; van Leusen, D.; Meetsma, A.; Hessen, B. *Organometallics* **1998**, *17*, 3645–3647. (d) Cardin, C. J.; Cardin, D. J.; Morton-Blake, D. A.; Parge, H. E.; Roy, A. *Dalton Trans.* **1987**, *7*, 1641–1645.

Scheme 4. Transition States for the Markovnikov (I) and Anti-Markovnikov (J) Insertion of Propargylamine into a Zr–SR Bond



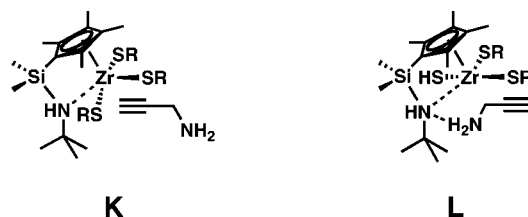
the radical inhibitor, γ -terpinene (Figure 2).⁵⁴ For example, the formation of anti-Markovnikov products in the **6** + **11** \rightarrow **12** transformation is suppressed by 10 \times through addition of the radical inhibitor (Figure 4). Furthermore, from the observation of greater Markovnikov selectivity with increased catalyst concentrations (Figure 5), it can be concluded that the organozirconium complex is not involved in radical generation or propagation processes, but rather Zr-centered catalytic turnover is in kinetic competition with the radical-mediated side reaction. Because the same anti-Markovnikov products are also observed in the absence of organozirconium complexes,⁵⁵ the radical process can clearly be initiated in the absence of the organometallic catalyst.

The present variation in Markovnikov selectivities for different substrates is found to be largely a function of the organometallic catalyst-mediated process competing with radical hydrothiolation.⁴ As is the case for substrate **13** (Table 2), low selectivity correlates with the inability of the sluggish catalytic reaction to effectively outrun the competing radical process. Other differences in selectivity result from varying substrate reactivities with respect to radical hydrothiolation. For example, conjugated alkynes (e.g., Table 3, entry 5) evidence lower hydrothiolation selectivities, possible the result of resonance stabilization of the postaddition radical intermediate.⁴

Because γ -terpinene addition does not appreciably suppress anti-Markovnikov products in the **34** + **11** \rightarrow **35** transformation, the low selectivity of CGCZrMe₂ (**1**)-catalyzed hydrothiolation of propargylamine (**34**) is unlikely the result of a radical side reaction. Preferential reduction in transition state energy by amine precoordination to the metal center⁵⁶ may contribute to the observed enhanced activity and reduced selectivity (Scheme 4); however, this fails to adequately explain the high selectivity observed with Cp*ZrBn₃ (**2**) as the catalyst. One possible explanation is hydrogen bonding between the amine functionality of substrate **34** and the CGC ligand HN group whereby the alkyne functionality is held in an anti-Markovnikov orientation⁵⁷ for subsequent insertion into the Zr–SR bond (Scheme 5, L).

Activation Parameters. Through variable temperature kinetic studies, the activation parameters for CGCZrMe₂ (**1**)-mediated **6** + **11** \rightarrow **12** are summarized below (Table 5, entry 1) along with previously reported activation parameters for analogous intramolecular and intermolecular hydrozirconation processes.

Scheme 5. Propargylamine (**34**) Orientations for the Formation of Markovnikov (K) and Anti-Markovnikov Products (L)



As is apparent below, the activation parameters for the present transformation generally parallel analogous insertions of unsaturations into L_nM–E (E = N, O, S) bonds where L_nM = a group 4 or f-element center. The larger ΔH^\ddagger compared to organozirconium-mediated hydroamination (Table 5, entry 4) is consistent with a stronger Zr–SR bond enthalpy imposing a greater barrier for insertion.⁵⁸ The negative ΔS^\ddagger indicates a highly ordered transition state; however, the magnitude is more consistent with intramolecular processes indicating reduction in the degrees of freedom as the insertive transition state is traversed.

Kinetics and Mechanism of Intermolecular Hydrothiolation of Terminal Alkynes. A summary of organozirconium-mediated alkyne hydrothiolation observables and kinetic data is presented below, as a prelude to further mechanistic discussion.

1. Empirical rate law: Rate = $k_{\text{obs}}[\text{Zr}]^1[\text{alkyne}]^1[\text{thiol}]^x$, $x = 0-1$
2. High Markovnikov selectivity
3. Observed zirconium–thiolate complexes present in the reaction media
4. Activity dramatically influenced by increased thiol encumbrance and moderately by alkyne encumbrance
5. Activation parameters consistent with turnover-limiting insertion processes
6. Alkyne isotopic labeling yields $k_{\text{H}}/k_{\text{D}} = 1.3(0.1)$
7. Single product isotopomer formation early in the reaction
8. Deuterium scrambling between alkyne and thiol
9. Gradual formation of multiple product isotopomers as the reaction progresses.

Rapid catalyst activation (i.e., Zr–Me and Zr–Bn bond cleavage) is observed with the addition of thiol as indicated by the formation of methane or toluene in the ¹H NMR. In deuterium-labeling studies with deuterated alkyne and nondeuterated thiol, the exclusive observation of CH₄ during CGCZrMe₂ (**1**) activation evidences that thiol-induced Zr–CH₃ protonolysis is operative and the exclusive or dominant pathway for catalyst activation under reaction conditions (eq 9). This is despite literature reported alkyne-mediated protonolysis^{39,52a} of similar Zr–C bonds and is quantified by thiol-mediated protonolysis measuring 150 \times faster than analogous alkyne-mediated protonolysis of Zr–Me bonds in the present study. In addition, the detection of zirconium–thiolate species in solution support a thiolate catalyst resting state, while observed zirconium–thiolate dimers in the reaction medium suggest instances of dimeric catalyst resting states and possible aggregated, hydrothiolation-active species.

The kinetics, deuterium labeling, observation of zirconium–thiolates, and the high degree of Markovnikov regioselectivity are consistent with an alkyne insertion pathway. This is analogous to organoactinide-mediated hydrothiolation,¹¹ where

(53) (a) Horton, A. D.; Orpen, A. G. *Organometallics* **1991**, *10*, 3910–3918. (b) Burger, B. J.; Thompson, M. E.; Cotter, W. D.; Bercaw, J. E. *J. Am. Chem. Soc.* **1990**, *112*, 1566–1577.

(54) γ -Terpinene is added in equimolar quantities to alkyne.

(55) Silva, M. S.; Lara, R. G.; Marczewski, J. M.; Jacob, R. G.; Lenardão, E. J.; Perin, G. *Tetrahedron Lett.* **2008**, *49*, 1927–1930.

(56) (a) Shen, H.; Chan, H.-S.; Xie, Z. *Organometallics* **2008**, *27*, 1157–1168. (b) Guerin, F.; McConville, D. H.; Vittal, J. J.; Yap, G. A. P. *Organometallics* **1998**, *17*, 5172–5177. (c) Walsh, P. J.; Hollander, F. J.; Bergman, R. G. *J. Organomet. Chem.* **1992**, *428*, 13–47.

(57) Shibasaki, M.; Yoshikawa, N. *Chem. Rev.* **2002**, *102*, 2187–2210.

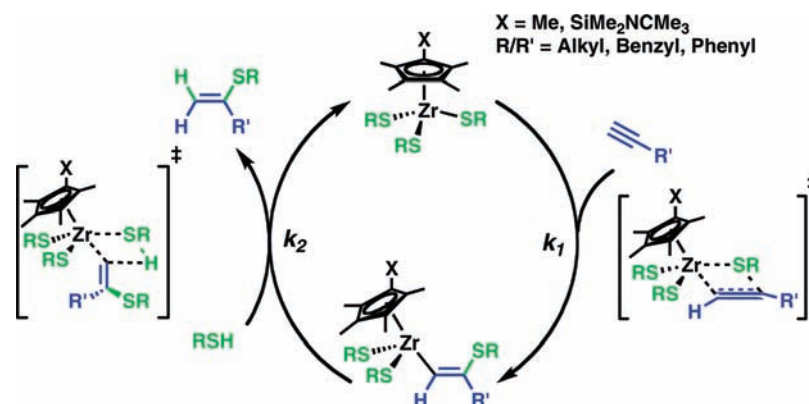
(58) Nolan, S. P.; Stern, D.; Marks, T. J. *J. Am. Chem. Soc.* **1989**, *111*, 7844–7853.

Table 5. Activation Parameters for Hydrothiolation, Hydroalkoxylation, and Hydroamination Processes

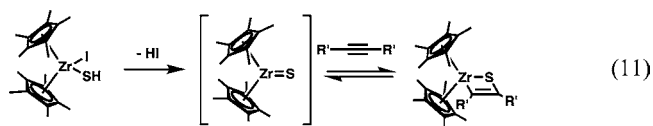
Entry	Metal	Reactants	Product	ΔH^\ddagger (kcal/mol)	ΔS^\ddagger (e.u.)
1	Zr			+18.1(1.2)	-20.9(2.5)
2 ^a	Th			+9.1(0.7)	-45(2)
3 ^b	U			+16(3)	-18(9)
4 ^c	Zr			+11(2)	-35(7)
5 ^d	Nd			+17.2(1.1)	-25.9(9)
6 ^e	La			+20.2 (1.0)	-11.8 (0.3)

^a Determined using $\text{Me}_2\text{SiCp}''_2\text{Th}(\text{CH}_2\text{TMS})_2$ as a precatalyst.¹¹ ^b Determined using $\text{CGCU}(\text{NMe}_2)\text{Cl}$ as a precatalyst.^{17b} ^c Determined using $\text{CGCZr}(\text{NMe}_2)\text{Cl}$ as a precatalyst.^{17b} ^d Determined using $\text{Me}_2\text{SiCp}''_2\text{NdCH}(\text{TMS})_2$ as a precatalyst.⁸¹ ^e Determined using $\text{La}[\text{N}(\text{TMS})_2]_3$ as a precatalyst.^{10k}

Scheme 6. Proposed Turnover-Limiting Alkyne Insertion Pathway for Organozirconium-Mediated Terminal Alkyne Hydrothiolation Mediated by a Representative Monomeric Organozirconium Complex⁶²



the acetylene undergoes insertion into the Zr–SR bond, followed by thiol-mediated protonolysis to yield product and regenerate the catalyst. Alkynes were previously reported to undergo π -bond metathesis with $\text{Zr}=\text{S}$ double bonds (eq 11)⁵⁹ to generate isolable species; however, $\text{C}=\text{C}$ insertion into a $\text{Zr}-\text{SR}$ σ -bond



has not, to the best of our knowledge, been reported until now. An equilibrium between a $\text{Zr}-\text{SR}$ σ -bond and an insertion-inactive $\text{Zr}(-)=\text{S}(+)\text{R}$ species similar to that observed with zirconium-phosphides⁶⁰ and in analogous organozirconium-mediated hydroamination^{8m,17b} can be envisioned. However the

necessity to maintain the $\text{C}-\text{S}$ bond^{61,44} requires the formation of a zwitterionic species, which is inconsistent with the negligible observed rate difference between ethanethiol (**7**) and 2,2,2-trifluoroethanethiol (**9**) hydrothiolation, despite different electronic characteristics. Therefore, we propose that the alkyne undergoes direct insertion into a $\text{Zr}-\text{SR}$ σ -bond with no competing $\text{Zr}-\text{S}/\text{Zr}=\text{S}$ equilibrium (Scheme 6, k_1).

In the hydrothiolation of **30-d**, the initial observation of product **31-DE** further supports an insertion pathway with subsequent thiol-mediated, protonolytic product formation (eq 12). Interestingly, deuterium exchange between the alkyne and

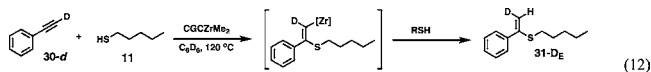
(59) (a) Carney, M. J.; Walsh, P. J.; Hollander, F. J.; Bergman, R. G. *Organometallics* **1992**, *11*, 761–777. (b) Carney, M. J.; Walsh, P. J.; Bergman, R. G. *J. Am. Chem. Soc.* **1990**, *112*, 6426–6428.

(60) Hou, Z.; Breen, T. L.; Stephan, D. W. *Organometallics* **1993**, *12*, 3158–3167.

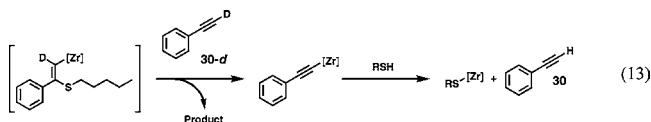
(61) Organozirconium complexes are known from the literature to cleave thiol C–S bonds; however, corresponding alkene products, indicative of this process, were not been observed by ¹H NMR or GC/MS.

(62) The catalytic cycle is presented here with a monomeric organozirconium complex for simplicity. See Supporting Information for a dimer catalytic cycle.

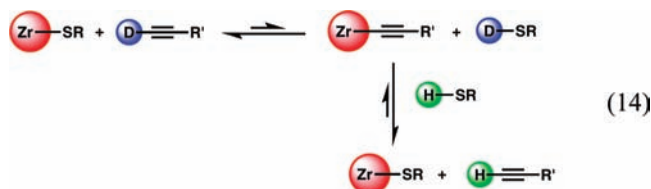
thiol as the reaction progresses eventually results in the formation products **31**, **31-D_Z**, and **31-D₂**. A control experiment



combining **30-d** and **11** without catalyst evidences no deuterium exchange, indicating that the scrambling of the isotopic labeling is zirconium-mediated and not a radical process. While alkyne-mediated protonolysis of the insertion product from the metal center is a possible source of deuterium migration to the alkyne (e.g., eq 13), this pathway is not believed significant since **1**-mediated deuterium swapping occurs between **15** and **30-d**



without observable insertion. Therefore, we propose that a zirconium-thiolate/zirconium-alkynyl protonolysis/deuterolysis side equilibrium is operative (e.g., eq 14). Because thiol-mediated Zr–C protonolysis is orders of magnitude faster than the analogous alkyne-mediated protonolysis and no zirconium-alkynyl⁶³ species is observed via NMR, this equilibrium is believed to strongly favor the zirconium-thiolate and is therefore kinetically insignificant to the catalytic cycle.



To test for a change in the turnover-limiting step in Scheme 6 when [thiol] > 0.3 M, variable temperature studies were performed with [thiol] at 1.2 M from 40 to 80 °C. The resulting activation parameters for [thiol] = 0.2 and 1.2 M are within modest margins of uncertainty, implying a common turnover-limiting step. This result thus supports a turnover-limiting alkyne insertion followed by a more rapid, thiol-mediated protonolysis at all investigated [thiol]. Regarding the interpretation of the kinetic data at lower [thiol], while the protonolysis is still more rapid than alkyne insertion, it is kinetically relevant to the overall rate of hydrothiolation. This situation is similar to an analogous lanthanide hydrophosphination^{9c,f–h} where protonolysis of intermediate metal–alkyl species is slow enough to be kinetically observable. With increasing [thiol] in the present case, the protonolysis is accelerated until alkyne insertion into the Zr–SR bond becomes the only kinetically relevant step of the overall reaction. This scenario can be modeled by the steady-state approximation (see Supporting Information for details) (eq 15) where alkyne insertion is turnover-limiting, where k_1/k_{-1}

are the rate constants for the insertion/extrusion of alkyne into the Zr–SR bond, and k_2 is the rate constant for thiol-mediated protonolysis of product from the metal center (see Scheme 6).⁶⁴ Consistent with the observed rate law (eq 8), the derived rate equation shows thiol and alkyne are approximately first-order at lower concentrations and the catalyst to be first-order at all concentrations. As [thiol] increases, the reaction rate remains first-order in catalyst and alkyne and becomes zero-order in [thiol] (Figure 6; eq 16). Alkyne does not become zero-order over the investigated concentration ranges since thiol protonolysis is far more rapid than alkyne insertion (i.e., $k_1 < k_2$) and k_{-1} is small. Equation 15 can be fit to Figure 6 with $k_1 = 7 \text{ h}^{-1} \text{ M}^{-1}$, $k_{-1} = 1 \text{ h}^{-1}$, and $k_2 = 20 \text{ h}^{-1} \text{ M}^{-1}$.

$$\text{Rate} = \frac{k_1 k_2 [\text{Zr}][\text{Thiol}][\text{Alkyne}]}{k_1 [\text{Alkyne}] + k_{-1} + k_2 [\text{Thiol}]} \quad (15)$$

$$\text{Rate} \approx k_1 [\text{Catalyst}][\text{Alkyne}] \text{ for } [\text{Thiol}] \gg [\text{Alkyne}] \quad (16)$$

Conclusions

The catalytic, organozirconium-mediated, intermolecular hydrothiolation of a wide range of terminal alkynes by aliphatic, benzylic, and aromatic thiols has been explored in terms of scope and mechanism. The ready availability of these zirconium complexes along with their high Markovnikov selectivities and efficacy with less reactive aliphatic thiols makes them an attractive alternative to many hydrothiolation catalysts. The activation parameters ΔS^\ddagger and ΔH^\ddagger were determined through variable-temperature studies and suggest a highly ordered transition state and an activation energy consistent with analogous hydroelementation processes. Based on kinetic data, the reaction is proposed to proceed through an alkyne insertion–thiol protonolysis sequence with turnover-limiting alkyne insertion.

Acknowledgment. The National Science Foundation (CHE-0809589) is gratefully acknowledged for financial support of this research. We also thank Dr. A. Atesin, Mr. S. Wobser, and Mr. M. Weberski for helpful discussions.

Supporting Information Available: Product characterization, kinetic equation derivations, NMR spectra, thermodynamic calculations, and kinetic data. This material is available free of charge via the Internet at <http://pubs.acs.org>.

JA103979B

- (63) (a) Ugolotti, J.; Kehr, G.; Fröhlich, R.; Grimme, S.; Erker, G. *J. Am. Chem. Soc.* **2009**, *131*, 1996–2007. (b) Albert, B. J.; Koide, K. *J. Org. Chem.* **2008**, *73*, 1093–1098. (c) Rosenthal, U.; Ohff, A.; Baumann, W.; Kempe, R.; Tillack, A.; Burlakov, V. V. *Angew. Chem., Int. Ed. Engl.* **1994**, *33*, 1605–1607.
- (64) Protonolysis is typically rapid in reports of organozirconium- and organo-f-element-mediated hydroelementation (refs 8h,n) but however, organolanthanide-catalyzed hydrophosphination (refs 9f–h) appears to have a more sluggish product protonolysis from the metal center, resulting in turnover-limiting protonolysis.